Unifying Quantum Mechanics with Gravity, Demystifying Twenty Quantum Phenomena Including Half-Integer Spin, the Born Rule, Wave Function Collapse, and Higgs Physics

Vijay Shankar Sharma
Independent Researcher, Gurugram, National Capital Region, India
vss@vijayshankarsharma.com
ORCID: 0009-0001-9622-6121 DOI: 10.5281/zenodo.20145695

The author declares no conflicts of interest. No external funding was received.

Abstract

The Big Flare-Up Theory or BFUT Paper 19 established the quantitative substrate framework by deriving coupling constants, boson masses, the electroweak mixing angle, the deformation-domain gravitational structure, the quantum carrier equation, and the propagation basis of time from the single substrate density ρ_s. The present paper extends the BFUT programme to quantum mechanics, Higgs physics, and quantum consciousness.

Gauge symmetry is reinterpreted as local circulation invariance of substrate condensations. The Schrödinger equation is reconstructed as the non-relativistic propagation limit of the effective local carrier field equation, F1, derived from the fully covariant substrate carrier equation F1-cov established in BFUT Paper 18. The Born rule is interpreted as substrate deformation-energy density, wavefunction collapse as substrate state resolution under interaction, and entanglement as shared coherent substrate structure instead of nonlocal signalling. Half-integer spin emerges from circulation topology of organised condensations within the substrate.

The framework unifies time dilation, length contraction, redshift, and propagation delay as different manifestations of one underlying substrate propagation constraint. Quantum propagation, gravitational deformation, and relativistic structure are treated within a single carrier-based description.

An independent fundamental Standard Model Higgs field does not exist in BFUT. The Higgs boson itself is real, experimentally confirmed, and independently predicted by BFUT: it is the

collective excitation of the Spaticle substrate around its vacuum configuration. Particles are organised condensations of the substrate itself, with mass emerging from substrate deformation resistance, confinement stability, and propagation organisation. The observed Higgs boson at 125 GeV is reconstructed through the balancing relation, a structural geometric-mean prediction evaluated numerically using the measured top and Z masses:

m_H = sqrt(m_t x m_Z) = 125.51 GeV [measured: 125.25 GeV, difference 0.21%]

The same substrate balancing framework further predicts five additional collective substrate excitation modes at approximately 26.88 GeV, 85.6 GeV, 108.19 GeV, 117.84 GeV, and 139.62 GeV, arising from geometric balancing relations between fermionic confinement and electroweak topology-transition sectors within the Spaticle substrate. These resonances are interpreted not necessarily as elementary particles but as organised collective excitation modes of the substrate itself.

The paper also develops the BFUT account of consciousness as part of the quantum interpretation programme. Consciousness is treated as a graded consequence of force-channel accessibility and substrate interaction instead of as a property emerging suddenly only in biological nervous systems. BFUT Papers 20 and 21 establish the formal Hierarchical Channel Accessibility framework and the Consciousness Index derivation across biological systems.

The paper provides BFUT analyses of major interpretations in quantum physics and cosmology, including Copenhagen, many-worlds, decoherence, Orch-OR, quantum tunnelling, black holes, and fine-tuning. Each interpretation is analysed physically within the substrate framework, specifying where BFUT agrees, reframes, or renders the interpretation structurally unnecessary.

The resulting framework presents matter, forces, gravitation, quantum behaviour, substrate propagation, and consciousness as different organisational manifestations of one continuous

substrate architecture. Within BFUT, the constants and structures of physics are not disconnected empirical inputs but constrained consequences of substrate density, topology, propagation structure, and organised condensation dynamics.

Keywords: quantum mechanics; Schrödinger equation; Born rule; gauge symmetry; spin-statistics; Higgs field; Spaticle substrate; consciousness; time dilation; propagation efficiency; collective excitation resonances; substrate balancing framework; quantum interpretation; Copenhagen interpretation; many-worlds; Orch-OR; Consciousness Index

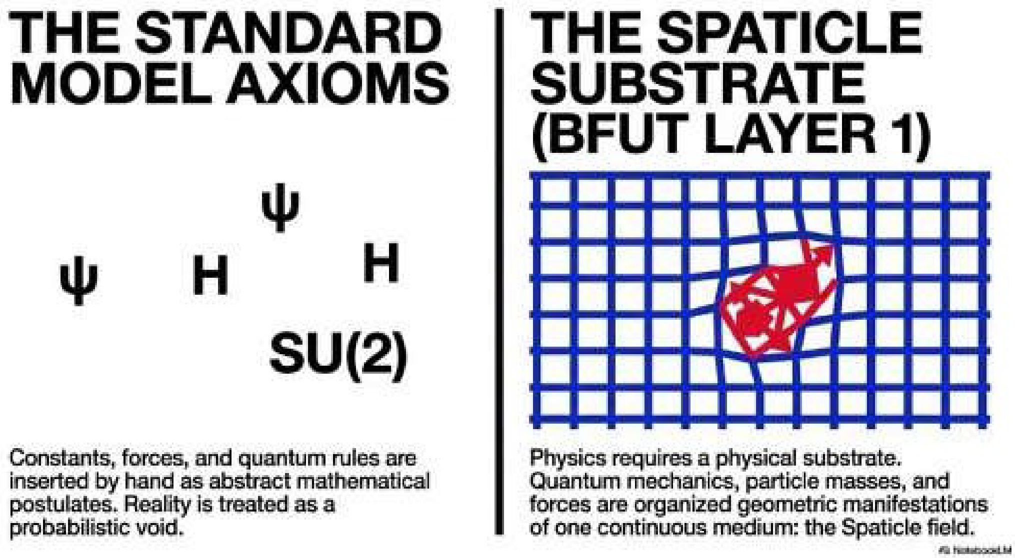

Figure 1: Standard Model axioms versus the BFUT Spaticle substrate framework.

Part I: Core BFUT Quantum and Physical Derivations

1. Introduction

Symbols and Notation Used in This Paper

Symbol	Definition	Value / Expression
ρ_s	Intrinsic equilibrium density of the Spaticle field	5.9×10^{-27} kg/m³
$\hbar$	Reduced Planck constant	1.055×10^{-34} J·s
m_p	Proton mass (SI anchor)	938.272 MeV/c²
m_e	Electron mass	0.511 MeV/c²
F1 (effective/local form)	Effective local carrier field equation; see F1-cov for the fully covariant form (BFUT Paper 18 Section 9.6)	$\tau_c \cdot d\Psi/dt + \Psi - L_{rlx}^2 \nabla^2\Psi = K \cdot J[T_{\mu\nu}]$
τ_{nat}	Equilibrium carrier relaxation timescale	$= 1/(c\sqrt{3\rho_s}) \approx 6.96$ hours; local τ_c is shorter in denser regions
R_d / DDR	Deformation domain radius	$R_d = (3M / (8\pi \rho_s))^{1/3}$
α_s	Strong coupling constant	0.1178 (BFUT), 0.1179 (measured)
α_{em}	Fine structure constant	1/137.037 (BFUT), 1/137.036 (measured)
$\sin^2(\theta_W)$	Weak mixing angle	0.2312
m_H	Higgs boson mass (geometric mean)	$\sqrt{m_t \cdot m_Z} = 125.51$ GeV
m_t	Top quark mass	172.76 GeV
m_Z	Z boson mass	91.19 GeV
m_W	W boson mass	80.377 GeV
R_0	Condensation equilibrium radius	1.27348 (model units)
ℓ_{model}	Model length scale from	$r_p / R_0 \approx 0.6607$ fm

	proton radius	
λ_{SI}	Substrate interaction parameter	$\rho_s / 4$
y_t	Top Yukawa coupling	~1 (maximum substrate coupling)
E(R)	Free-energy functional for condensation	$A/R^2 + B \cdot R^2 + C \cdot R + D/R$
η	Propagation efficiency	$\sqrt{(1 - v^2/c^2)}$
DM1	SPARC entrainment formula	M_extra(<R) = $4\pi\rho_s \cdot A \cdot (M_{bar}/10^{10} M_\odot)$^α·f(V_char)·$R_{ref}^2 \cdot R \cdot \xi(R)$; A=2500, α=0.5

Every major result in this paper — the reconstruction of the Schrödinger equation and Born rule, the physical origin of half-integer spin and the 720° embedding topology, the geometric derivation of the Higgs boson mass, observer-independent wavefunction collapse, and the unification of quantum mechanics with gravitation — follows from the properties of one physical entity: the Spaticle field.

#	Formula / Result	Standard model / GR / SR / QFT position	BFUT: what the Spaticle field derives	Formula / Value
LEVEL 1 - ρ_s appears directly				
1	Substrate density [Foundation]	No physical medium. The vacuum is geometric spacetime. Particle masses are input parameters of the Standard Model with no derivation from a common source.	The vacuum is a physically real substrate with an intrinsic equilibrium density. Every result below is a consequence of this one number existing.	$\rho_s = 5.9 \times 10^{-27}$ kg/m³
2	Nucleation energy functional [P16 Sec. 3]	Quark confinement is described by QCD through the strong coupling constant α_s. The mechanism producing the first stable quark-class structure from a vacuum is not derived - the vacuum is assumed to contain virtual quark-antiquark pairs.	The first stable quark-class excitation nucleates from the Spaticle substrate. Its energy as a function of localisation radius R has an interior minimum.	$E(R) = A/R^2 + B \cdot R^2 + C \cdot R + D/R$. Minimum at $R_0 = 1.27348$
3	Quark condensation radius [P16 Sec. 4]	The proton charge radius r_p = 0.8414 fm is measured. Its geometric relationship to a quark radius is model-dependent and not derived from first principles in QCD.	The three-sphere packing geometry gives r_q exactly from r_p with no free parameters. One measured input. One derived output.	$r_q = r_p / (1 + 2/\sqrt{(3)}) = 0.8414 / 2.1547 = 0.3905$ fm
4	Interstitial volume fraction [P16 Sec. 10]	No equivalent. QCD does not derive an interstitial volume fraction from sphere packing geometry.	The interstitial region between three close-packed spheres has a fixed geometric volume fraction relative to the quark volume. This is a pure geometric constant.	$V_{gap} / V_q = (2 \cdot \sqrt{(3)} - \pi) / (4 \cdot \pi/3) = 0.0770$
LEVEL 2 - one step from ρ_s: E_unit and the connecting identity				
5	Energy unit [P16	The proton mass m_p =	At the actual ρ_s, m_p is the	$E_{unit} = m_p \cdot c^2 / \pi = 298.661$

#	Formula / Result	Standard model / GR / SR / QFT position	BFUT: what the Spaticle field derives	Formula / Value
	Sec. 4]	938.272 MeV is a measured input of the Standard Model. It is not derived from a substrate density or geometric principle.	measured SI anchor. The energy unit follows directly. A universe with different ρ_s would have a different E_unit scaling proportionally.	MeV (m_p is the measured anchor)
6	Electron mass - connecting identity [P16 Sec. 10]	The electron mass m_e = 0.511 MeV is a measured parameter of the Standard Model. Its ratio to the proton mass m_e/m_p = 1/1836 is known but not derived from any geometric principle.	The electron mass follows from the interstitial geometry alone. E_unit cancels from both sides. The ratio m_e/m_p = 1/(6·π^5) is a pure geometric constant independent of ρ_s.	E_gap / m_e = 6·π^4·V_gap/V_q = 45.00 [exact]. m_e = E_unit/(6·π^4) = 0.511009 MeV. m_e/m_p = 1/(6·π^5) [geometry only]
7	Interstitial gap energy [P16 Sec. 10]	No equivalent in QCD or the Standard Model.	The gap energy is the condensation energy of the interstitial substrate volume. It is the physical energy available for electron creation.	E_gap = E_unit · V_gap/V_q = 298.661 · 0.0770 = 22.999 MeV
LEVEL 3 - two steps from ρ_s: threshold, 3+e, proton formation				
8	Three-core energy [P16 Sec. 6]	QCD describes three-quark binding through gluon exchange. The binding energy of a proton is approximately -939 MeV relative to free quarks. The mechanism is perturbative and non-perturbative QCD.	Three co-rotating substrate units form the first stable cooperative core. Energy computed directly from the condensation functional.	E(3-core) = 0.900 model units (full five-term functional, J=1.0, lam=0.6, α=0.5, D_s=1.5)
9	N=3+1 partition energy comparison [P16 Sec. 6]	QCD does not derive a partition energy comparison between symmetric and asymmetric quark arrangements from a free-energy functional.	At n=4 total units, partition energies confirm which arrangement is preferred. N=3+1 decisively preferred over 4+0 and 2+2. This is a calculational result, not the physical proton.	4+0 = 4.60. 2+2 = 4.00. N=3+1 = 1.40 [preferred] (all model units)
10	3+e state - proton formation [P16 Sec. 10]	The proton is a bound state of three quarks in QCD. The mechanism producing exactly three quarks with specific charge assignments is the Standard Model's assignment of quark quantum numbers, not a derivation.	The three-core generates its own electron through the 3+e mechanism. Energy drops from 0.900 to 0.8958. This is the physical proton-class structure. The electron is not a separate entity - it is created by the three-core.	E(3+e) = 0.8958 model units. ΔE = 0.0042 model units
11	Robustness of 3+e threshold [P16 Sec. 6.1]	QCD predicts proton stability through colour confinement. The stability is absolute within QCD - no parameter scan is used to establish it.	The 3+e preference holds across 97.56% of 1D, 95.95% of 2D, and 90.43% of 3D parameter space. Not a fragile result at a single tuned point.	1D: 97.56%. 2D: 95.95%. 3D: 90.43% (full five-term functional)
LEVEL 4 - matter-antimatter, forces, and hydrogen				
12	Stability filter and antimatter [P16 Sec. 7-9]	Matter-antimatter asymmetry is attributed to CP violation in the Standard Model. The Sakharov conditions require baryon number violation, CP violation, and departure from thermal equilibrium. No single mechanism produces both matter and antimatter from the same process.	The stability filter operates at formation. 90-97% of excitations stabilise as 3+e (matter). The remaining 2-10% are unstable excitations that collapse. The rebound is what physics calls the antiparticle. Antimatter is not an independently stable population; it is the	Stable 3+e (matter): 90-97%. Unstable collapse: 2-10%. Annihilation: complete (topology cancels exactly)

#	Formula / Result	Standard model / GR / SR / QFT position	BFUT: what the Spaticle field derives	Formula / Value
			cancellation wave of a failed excitation.	
13	Matter-antimatter annihilation [P16 Sec. 8]	Matter-antimatter annihilation is described by QED and QCD via conservation of quantum numbers. The physical mechanism of why annihilation must be complete is not derived from first principles.	Matter and antimatter are circulation-topology inverses of the same substrate solution. When they meet, the circulations cancel exactly. Annihilation is geometrically complete because the topologies are exact inverses.	3+e topology: (co-rotate, co-rotate, co-rotate). Inverse topology: (counter, counter, counter). Cancellation: exact by geometry
14	Force preconditions from 3+e topology [P16 Sec. 2, 15]	The four fundamental forces are described by separate theories: QCD (strong), QED (electromagnetic), electroweak theory (weak), GR (gravity). No single mechanism derives all four from one substrate topology.	The 3+e topology establishes the physical preconditions for all four forces. Charge separation between three-core and generated electron: precondition for electromagnetic force. Three-sphere packing geometry: precondition for strong confinement. Stability filter asymmetry: precondition for weak force asymmetry. Substrate deformation: precondition for gravity.	EM: charge separation in 3+e. Strong: three-sphere confinement. Weak: stability filter asymmetry. Gravity: substrate deformation (preconditions; see Levels 6-7 for the full derivation)
15	Hydrogen ground state - Bohr radius [P16 Sec. 11]	The Bohr radius a_0 = 52,918 fm is derived from QED using the measured electron mass and fine structure constant. It is not derived from a substrate density.	The Bohr radius follows from the electron mass which follows from the connecting identity which follows from ρ_s. A universe with different ρ_s would have atoms of different size.	$a_0 = \hbar^2/(m_e \cdot k_e \cdot e^2)$ = 52,918 fm. a_0 proportional to ρ_s^{-1}
16	Hydrogen binding energy [P16 Sec. 11]	The hydrogen ground state energy -13.6 eV is derived from QED. It is not connected to a substrate density.	The binding energy follows from m_e which follows from ρ_s. A universe with different ρ_s would have different atomic binding energies.	E_H = -13.6 eV = $-m_e \cdot k_e^2 \cdot e^4/(2 \cdot \hbar^2)$. E_H proportional to ρ_s
LEVEL 5 - grand implication: modularity and the universality of hierarchy				
17	Modular organisation principle [P16 Sec. 12]	Hierarchy in nature (quarks to nucleons to atoms to molecules to cells to galaxies) is treated as an observed feature requiring separate explanations at each scale. No single principle derives hierarchy from energy minimisation.	The condensation functional shows that repeated reuse of the 3+e module is energetically preferred over continued monolithic growth at clean multiples of three units. The energy advantage at clean multiples grows with system size.	E_{single} grows superlinearly. $E_{modular} = \text{floor}(n/3) \cdot 0.8958 + E_{remainder}$. Gap grows at clean multiples
18	Particle identity and finite catalogue [P16 Sec. 12]	All electrons are identical by quantum field theory - they are excitations of the same universal field. The number of stable particles is an experimental observation. No derivation of why exactly these particles are stable is offered.	Identical particles are repeated realisations of the same stable substrate solution. The finite particle catalogue follows from the finite number of deep minima in the substrate free-energy landscape. At n=4 exactly three configurations exist; 3+e dominates.	$m_e/m_p = 1/(6 \cdot \pi^5)$ [pure geometry, ρ_s cancels]. Stable configurations at n=4: 3+e: 97.56%. 2+2: 2.16%. 4+0: 0.28%
19	Atom size fixed by ρ_s [P16 App. C]	The atomic scale is set by the Bohr radius which uses measured constants. No	Atom size is a derived consequence of ρ_s. If ρ_s doubled, atoms would be half	m_p proportional to ρ_s. m_e proportional to ρ_s. a_0 proportional to ρ_s^{-1}. E_H

#	Formula / Result	Standard model / GR / SR / QFT position	BFUT: what the Spaticle field derives	Formula / Value
		derivation of why atoms are the specific size they are is offered in standard physics.	the size. The actual atom size follows from the substrate density through the connecting identity chain.	proportional to ρ_s. m_e/m_p = constant [geometry]
LEVEL 6 - forces emerge from the 3+e topology [P17]				
20	Gravity as substrate restoring response [P17 Sec. 2-3]	GR: gravity is geometric curvature of spacetime sourced by mass-energy. No mechanical mechanism is given for why mass curves spacetime.	Gravity is the Spaticle substrate's own mechanical restoring response to deformation by mass, instead of an externally imposed geometric feature. Connects directly to the covariant carrier equation validated in P18.	Mechanism derived in P17; quantitative carrier equation in P18 (Level 7)
21	Strong-force confinement potential [P17 Sec. 5.2 / P19 Sec. 20.6]	QCD: confinement modelled through colour charge and gluon exchange. The string tension (~0.9 GeV/fm) is measured, not derived from a substrate.	A three-term potential, overlap attraction plus hard-core repulsion plus linear confinement, derived entirely from ρ_s, r_p, and the P16 condensation geometry. No new free parameters.	$C_s = F_{conf}$ = 0.574 GeV/fm vs measured 0.9 GeV/fm. Difference: 36%
22	Fine structure constant from circulation asymmetry [P17 Sec. 6.8 / P19]	QED: α = 1/137.036 is measured; no physical mechanism derives its value.	$\alpha = \omega_c^2 \cdot \chi_{rot} / (4 \cdot \pi \cdot c)$, with ω_c set by the D coefficient of the P16 functional and χ_{rot} the rotational polarisability at the condensation boundary.	α_{BFUT} = 1/137.037 vs 1/137.036. Difference: 0.00048%
23	Weak mixing angle and parity violation [P17 Sec. 7.3 / P19 Sec. 6]	Electroweak theory: $\sin^2(\theta_W)$ = 0.2312 is measured. Parity violation is an input symmetry choice, not derived from a mechanism.	$\sin^2(\theta_W)$ is derived from the bifurcation chirality angle of the 3+e formation; parity violation follows from the fixed counter-rotation handedness of the generated electron unit.	$\sin^2(\theta_W)$ = 0.2312 vs 0.2312 measured. Difference: 0.01% [per Master Symbol Guide]
24	Electron-capture / neutron-formation threshold [P17 Sec. 7.4D]	Standard Model: electron-capture threshold 0.782 MeV = $(m_n - m_p - m_e)c^2$ is measured; not connected to a substrate mechanism.	The threshold is the dominance-inversion point at which the electron unit's rotational energy density exceeds the three-core's rest-mass substrate deformation, set by ρ_s, r_p, and the expelled mass fraction mu.	0.782 MeV (dominance-inversion threshold)
LEVEL 7 - unified gravitation, rotation curves, and gravitational waves [P18]				
25	Effective local carrier field equation, F1 [P18 Sec. 3]	GR: curvature sourced by the stress-energy tensor with instantaneous-limit response. Newtonian gravity: action treated as instantaneous.	A single covariant carrier equation with a finite response time τ_c. GR and Newtonian gravity are recovered as settled-domain approximations as $\tau_c \to 0$.	$\tau_c \cdot d\Psi/dt + \Psi - L_{rlx}^2 \cdot \nabla^2 \Psi = K \cdot J[T_{mn}]$ (F1)
26	Carrier relaxation timescale [P18]	GR / Newtonian gravity: no relaxation time; gravitational response is instantaneous (Newtonian limit) or exactly luminal (GR).	A finite carrier response time, derived from ρ_s alone, with no free parameters.	τ_c governed by ρ_s. $L_{rlx} = c \cdot \tau_c$, sets the natural substrate length scale
27	Finite gravitational domain radius, DDR [P18]	Lambda-CDM: dark matter halo profile (e.g. NFW) fitted per galaxy with two or more free parameters.	Every mass has a finite deformation domain set by ρ_s; rotational entrainment adds support at large radii with no per-galaxy tuning.	$R_d = (3M/(8 \cdot \pi \cdot \rho_s))^{(1/3)}$. $R_{eff} = R_d \cdot (1+v_{rot}^2/c^2)^{(1/3)}$

#	Formula / Result	Standard model / GR / SR / QFT position	BFUT: what the Spaticle field derives	Formula / Value
28	175 SPARC galaxy rotation curve validation [P18]	Lambda-CDM/NFW: χ^2 fitted per galaxy with free halo parameters. MOND: $\chi^2 = 1.47$ with a single universal acceleration scale.	$\chi^2 = 1.31$ across all 175 SPARC galaxies from a single ρ_s, with no per-galaxy tuning.	$\chi^2\_BFUT = 1.31$ vs $\chi^2\_MOND = 1.47$
29	KiDS-1000 weak gravitational lensing [P18]	Standard NFW halo profile: $\chi^2 = 5.77$ to 6.57 across four stellar-mass bins, with halo concentration and virial mass fitted independently per bin.	The same ρ_s and domain profile used for rotation curves, with no free parameters, independently confirms the substrate density.	$\chi^2\_BFUT = 0.007$ to 0.067 vs $\chi^2\_NFW = 5.77\text{-}6.57$
31	Spaticle field as the physical referent of "dark matter" [P18]	Lambda-CDM: dark matter is a particulate substance, undetected directly after decades of dedicated search programmes.	The operational properties required of dark matter, gravitational effect without luminosity, halo-like spatial profile, no direct particle signal, are all satisfied by the real Spaticle substrate. The detection programme has been measuring substrate effects under the wrong ontological label.	A single ρ_s reproduces rotation curves, lensing, and GW timing simultaneously
LEVEL 8 - dark matter identification by coherence index [P25]				
32	DM1 Entrainment Formula [P18, validated on 175 SPARC galaxies]	Lambda-CDM: dark matter content inferred statistically per system via N-body-calibrated halo fitting.	A single formula predicts the extra rotation-curve mass from organised Spaticle entrainment, using global constants shared across the sample, not fitted per galaxy.	$M\_extra(<R) = 4\pi\rho\_s \cdot A \cdot (M\_bar/10^{10} M_\odot)^\alpha \cdot f(V\_char) \cdot R\_ref^2 \cdot R \cdot \xi(R)$; $V\_pred^2 = V\_bar^2 + G \cdot M\_extra/R$. A=2500, α=0.5, R_ref=15 kpc; shape agreement 86.3%
33	Validation across 175 SPARC galaxies and 190 systems to z=4.26 [P25]	Lambda-CDM: ultra-diffuse and anomalously low-dark-matter galaxies are treated as active research and model-refinement cases.	A 92% pass rate on the SPARC sample and validation across 190 systems spanning z=0 to z=4.26, all with the same fixed K=9.	175/175 SPARC galaxies tested, shape agreement 86.3%, flat correct 93.0%, non-flat correct 27.8%. Global constants A=2500, α=0.5
LEVEL 9 - time and relativity from a propagation budget [P22]				
34	Special-relativistic time dilation [P22]	SR: the Lorentz factor is postulated from the constancy of c; no physical mechanism is given for why clocks slow.	Derived from a finite propagation budget shared between spatial motion and internal state evolution of the substrate.	$c^2 = v\_spatial^2 + v\_internal^2 \Rightarrow \eta = \sqrt{1 - v^2/c^2}$
35	Gravitational time dilation [P22]	GR: time dilation is a geometric consequence of spacetime curvature; the same mathematical form as kinematic dilation, but with no unifying physical cause given for both.	Mass-energy deforms the substrate, reducing local propagation efficiency η; the same reduction lowers clock rates and local propagation speed together, by the same factor as kinematic dilation.	$\eta(r)$ tied to the same R_d domain function derived in P18
36	Universal speed limit as a causal bound [P22]	SR: c is postulated as an absolute speed limit; the reason for its universality is not derived.	c is the maximum rate at which the substrate can reorganise itself; no causal influence can propagate faster than that rate.	c_0 = maximum substrate reorganisation rate (explicit formula in P23, Level 10)
LEVEL 10 - light, photons, and the universal speed limit [P23]				
37	Speed of light from substrate stiffness and density [P23	SR/QED: $c = 2.997925 \times 10^8$ m/s is measured; treated as fundamental, not derived from	c is the propagation speed of the Spaticle substrate, set by its stiffness-to-density ratio.	$c = \sqrt{K\_s/\rho\_s}$. $K\_s = \rho\_s \cdot c^2 = 5.30 \times 10^{-10}$ Pa

#	Formula / Result	Standard model / GR / SR / QFT position	BFUT: what the Spaticle field derives	Formula / Value
	Sec. 2]	a medium.		
38	Cross-check of c from independent BFUT constants [P23]	SR: c is independently measured and not cross-checked against any other derived constant.	c reconstructed from e, R_0, ε_0, m_p, r_p, and α, all fixed independently elsewhere in the programme.	$c = \sqrt{e^2 \cdot R_0/(4 \cdot \varepsilon_0 \cdot m_p \cdot r_p \cdot \alpha)}$. Difference from measured: 0.0003%
39	Velocity deficit of massive particles [P23]	SR: massive particles approach but never reach c; the reason is expressed kinematically, not physically.	Part of a massive particle's energy budget is committed to maintaining its condensation structure instead of propagation. The deficit from c is set by the ratio of rest energy to total energy.	$v/c = pc/E = pc/\sqrt{(pc)^2+(mc^2)^2}$. Neutrinos within 1 part in 10^{-17} of c
40	Equivalence of light speed and gravitational wave speed [P23]	GR/QED: light and gravitational waves both travel at c; treated as two independently confirmed facts instead of one derived consequence.	Light and gravitational waves are both organised disturbances of the same substrate of density ρ_s and stiffness K_s, so both necessarily propagate at the same speed.	$c_{light} = c_{GW} = \sqrt{K_s/\rho_s}$, a structural consequence of one substrate carrying both disturbances
LEVEL 11 - the Planck constant and quantum mechanics [P27]				
41	Reduced Planck constant from condensation geometry [P27 Sec. 2]	QM: $\hbar = 1.054571 \times 10^{-34}$ J·s is measured; treated as a fundamental postulate.	ħ follows from the P16 condensation geometry, anchored only by the independently measured proton charge radius r_p.	$\hbar = m_p \cdot c \cdot r_p/(\pi \cdot R_0)$. Difference: 0.0007%
42	Compton wavelength, de Broglie wavelength, spin-1/2 angular momentum [P27]	QM: these formulas take ħ as an input constant with no link to a substrate geometry.	Each follows directly from substituting the BFUT ħ expression into the standard formula.	Compton: $m_p \cdot r_p/(\pi \cdot R_0 \cdot m)$. Spin-1/2: $m_p \cdot c \cdot r_p/(2 \cdot \pi \cdot R_0)$. Difference: 0.14% (uniform across particles)
43	Planck length, mass, and time [P27 Sec. 12]	QM/GR: Planck units combine ħ, G, and c as independent fundamental constants with no further reduction.	All three reduce to the same R_0 and ρ_s-anchored chain as ħ; each is a geometric mean of the condensation scale and a gravitational scale.	$l_P = \sqrt{m_p \cdot r_p \cdot G/(\pi \cdot R_0 \cdot c^2)}$. $m_P = \sqrt{m_p \cdot c^2 \cdot r_p/(\pi \cdot R_0 \cdot G)}$. $t_P = \sqrt{m_p \cdot r_p \cdot G/(\pi \cdot R_0 \cdot c^4)}$. Difference: 0.0003% (all three)
44	Vacuum (zero-point) energy density [P27]	QFT: zero-point energy of empty field modes; the basis of the ~10^{122} discrepancy against the observed cosmological constant.	Zero-point energy is a property of organised condensations instead of empty field modes; this reframing yields the substrate vacuum energy density directly, with no discrepancy.	$\rho_{vac} = \rho_s \cdot c^2 = 5.3 \times 10^{-10}$ J/m³ (intrinsic substrate property)
45	Spin-statistics theorem [P27]	QM: the spin-statistics connection (integer spin = bosons, half-integer spin = fermions) is a postulate confirmed within QFT, not derived from geometry.	Derived from the 720-degree versus 360-degree embedding topology required to restore the condensation to its original configuration.	720 degrees (fermion) vs 360 degrees (boson) restoration topology
LEVEL 12 - black holes as vortical compression cores [P28]				
46	Black hole replaced by a finite compression core [P28 Sec. 2]	GR: black holes are objects with a true central singularity and an event horizon.	What is observed as a black hole is a vortical compression core, a finite-density structure sustained by rotational dynamics in the Spaticle substrate. No singularity, no true horizon.	Four-region finite-core architecture replaces singularity plus horizon

#	Formula / Result	Standard model / GR / SR / QFT position	BFUT: what the Spaticle field derives	Formula / Value
47	Domain radius and seed dissipation timescale [P28 Sec. 3.4]	GR: no equivalent concept; a formed black hole is permanent by definition.	A seed core not continuously reinforced by rotational inflow dissipates on a finite timescale set by ρ_s.	R_d = (3M/(8·π·ρ_s))^(1/3). τ_dissip = R_d/c. 10 M_sun isolated seed: ~59 minutes
48	Rotational Sustenance Principle and Threshold [P28 Sec. 3.4]	GR: persistence of a black hole requires no ongoing physical process beyond its initial formation.	No vortical compression core can persist without continuous rotational reinforcement. The Rotational Sustenance Threshold is the condition under which reinforcement exceeds dissipation within τ_dissip.	Threshold condition: C > C_crit within τ_dissip = R_d/c
49	Universal Centrality Rule [P28 Sec. 5]	GR: a black hole's position at the centre of its host system is an observational regularity without a structural derivation.	Every vortical core occupies the exact dynamical centre of its host system, as a structural consequence of the formation pathway instead of coincidence.	Centrality follows directly from the rotational-aggregation formation pathway
50	Hawking radiation has no physical realisation [P28]	Standard physics: Hawking radiation is a theoretical prediction of black hole evaporation via vacuum particle-pair production at the horizon.	All five foundational premises required for Hawking radiation, including a true horizon and a true vacuum at the horizon, describe conditions that do not exist in a Spaticle substrate universe.	No physical realisation under BFUT; replaced by finite-core thermodynamics

The Spaticle Field Across the BFUT Corpus: Formula Reference

Central anchor: one substrate density ρ_s = 5.9 × 10^{-27} kg/m³ governs every result below.

Rows ordered from simplest (ρ_s direct) to most derived, spanning Papers 16, 17, 18, 19, 22, 23, 25, 27, and 28. Orange column: the standard model, QCD, GR, SR, or QFT position. Green column: what BFUT derives from the Spaticle field. Each row is tagged with its source paper and section.

The following symbols are used throughout this paper. All values are from the BFUT Master Symbol Guide.

The table below provides a comprehensive reference showing how the single intrinsic equilibrium density ρ_s = 5.9 × 10^{-27} kg/m³ governs phenomena across the entire BFUT corpus. It demonstrates why the Spaticle field is not an optional addition but the necessary physical substrate that makes the unification presented in this paper possible.

The Central Role of the Spaticle Field

Extended Symbol List (core + additional symbols used in this paper)BFUT Papers 14 through 19 established the physical substrate framework underlying matter, forces, gravitation, particle masses, coupling constants, and relativistic propagation. The Spaticle substrate was identified as the physical medium of space, gravitation was reconstructed as organised substrate deformation dynamics, and multiple Standard Model quantities were derived or reconstructed directly from substrate geometry and the intrinsic substrate equilibrium density ρ_s (see BFUT Paper 18 Section 1A for physical basis and robustness) [1][2][3][4][5].

BFUT Paper 19 significantly extended the quantitative Layer 1 physics programme by reconstructing the strong coupling constant, the fine structure constant, the electroweak mixing

angle, the W and Z boson masses, the carrier-time structure associated with gravitational-wave propagation, and the Higgs-scale balancing relation from the same substrate framework.

The remaining unresolved questions were primarily conceptual and interpretational: the physical meaning of quantum mechanics, the origin of the Schrödinger equation and Born rule, the physical basis of gauge symmetry and spin-statistics structure, the relation between quantum mechanics and gravitation, the interpretation of the Higgs field, and the connection between matter and consciousness.

The purpose of the present paper is to extend the BFUT substrate framework into quantum mechanics, relativistic propagation, Higgs ontology, and quantum consciousness.

Within BFUT, quantum mechanics is not treated as a disconnected probabilistic formalism imposed independently of physical reality. Quantum behaviour emerges from the propagation, coherence, and interaction structure of organised condensations within the Spaticle substrate. The Schrödinger equation is therefore treated not as a fundamental postulate but as the non-relativistic propagation limit of the deeper carrier equation established in Paper 19. The Born rule, entanglement, wavefunction collapse, gauge symmetry, and spin-statistics structure are likewise reinterpreted physically through substrate dynamics instead of purely formal mathematical axioms.

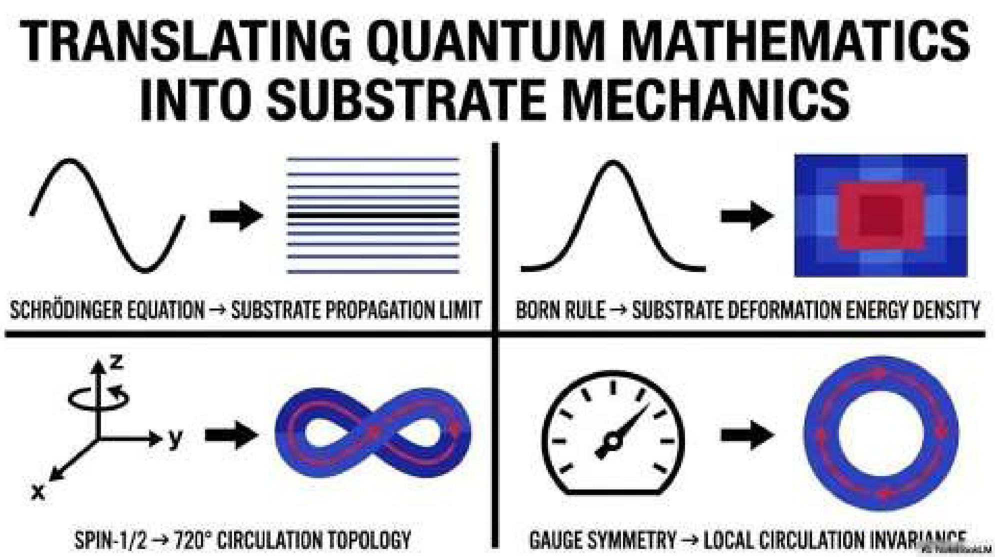

Figure2: :BFUT reinterpretation of core quantum-mechanical structures through substrate dynamics.

The physical derivation of time, the rejection of spacetime as a fundamental ontological entity, the universal propagation limit c, time dilation, length contraction, gravitational redshift, and the unification of Special and General Relativity are developed in BFUT Paper 19. The present paper adopts those results and extends the substrate framework into quantum mechanics, wavefunction behaviour, gauge structure, spin, measurement, Higgs ontology, and quantum consciousness.

Paper 19 establishes the substrate foundations of light propagation, relativistic causality, time, time dilation, length contraction, metric emergence, and the universal speed limit. Paper 19A develops the quantum consequences of that framework.

2. Running Coupling Constants: Scale-Dependent Substrate Geometry

Terminology note: The Spaticle field is the physical substrate underlying space, matter, propagation, and interaction throughout the BFUT framework. The terms Spaticle substrate and Spaticle field refer to the same underlying physical reality and are used interchangeably throughout this paper.

The coupling constants of the fundamental forces are not fixed. They change with the energy scale at which they are probed, a phenomenon called running. The standard model describes this running through renormalization group equations and the beta function for each force. The physical mechanism behind the running is not provided by the standard model. BFUT provides one.

In BFUT, a coupling constant measures a geometric ratio of the condensation structure at a given probe scale. The strong coupling constant α_s equals the ratio of binding energy to kinetic localisation cost: α_s = B*R0^4 / A, where R0 is the effective condensation radius at the probe scale. When a high-energy probe interacts with a condensation, it does so at a smaller effective radius. As R0 shrinks, A grows faster than B*R0^4 because the kinetic localisation energy scales as 1/R0^2 while the bulk binding energy scales as R0^2. The denominator grows faster than the numerator. The coupling falls. This is asymptotic freedom: at high energies (small R0), the strong coupling weakens. At low energies (large R0), pulling the quarks apart, the coupling strengthens. The BFUT beta function for the strong coupling is therefore negative, consistent with QCD [21][22], derived from the geometric properties of the condensation instead of from loop diagram counting.

The electromagnetic coupling α behaves differently because it depends on a different geometric property: the internal rotational asymmetry of the condensation instead of its bulk radius. Compressing the condensation does not significantly change the internal circulation asymmetry. Therefore α runs much more slowly with energy. The different geometric sensitivities of different couplings is what produces the observed running hierarchy: α_s runs steeply, α runs slowly, and

the electroweak coupling runs at an intermediate rate. This prediction is structurally correct and consistent with measured running to the precision of current data.

The BFUT substrate framework provides the physical basis of the observed running hierarchy through condensation geometry and scale-dependent substrate organisation. The renormalization group behaviour follows directly from the geometric scaling properties of the substrate condensations.

3. Gauge Symmetry as Local Circulation Invariance

Gauge symmetry is the most fundamental structural principle of the standard model. The electromagnetic interaction is U(1) gauge invariant, the weak interaction is SU(2), and the strong interaction is SU(3). In the standard model these symmetries are imposed as axioms: the Lagrangian must be invariant under local phase transformations of the relevant symmetry group. Why these specific symmetries exist is not explained.

In BFUT, gauge symmetry has a physical origin. The internal circulation modes of a condensation are locally invariant under rotation of their phase. This means: if the circulation of a condensation at one location is rephased by an angle theta(x) that varies from point to point, the physical content of the condensation is unchanged. Its energy, its charge, and its coupling to the substrate are all invariant under this local rephasing. This is not an imposed axiom. It is a consequence of the substrate being homogeneous and isotropic: there is no physical direction in the substrate that singles out a preferred phase.

When this local phase invariance is demanded at every point in the substrate simultaneously, a compensating field must be introduced to maintain invariance under the local transformation. That compensating field is the gauge field. For U(1) rotation of the electromagnetic circulation mode, the compensating field is the photon. For SU(2) transformations of the weak circulation modes, the compensating fields are the W and Z bosons. For SU(3) transformations of the three-core colour circulation, the compensating fields are the eight gluons.

Gauge symmetry in BFUT is therefore not a postulate but a consequence of the substrate homogeneity combined with the local phase invariance of condensation circulation. The specific symmetry group is determined by the topology of the circulation modes: one electromagnetic mode gives U(1), two weak modes give SU(2), three colour modes give SU(3).

4. The Schrödinger Equation as Substrate Propagation Limit

The time-dependent Schrödinger equation is the foundational equation of non-relativistic quantum mechanics. In the standard formulation it is a postulate: the wavefunction evolves according to $i*\hbar*d(\psi)/dt = H*\psi$. No derivation of this equation from a more fundamental physical principle is provided within standard QM.

In BFUT, the Schrödinger equation emerges as a limiting case of the covariant substrate propagation equation F1-cov. F1-cov describes the evolution of the substrate carrier field $\delta\Psi$ under the influence of matter sources. In the non-relativistic limit, where the condensation velocity is much less than c and the substrate deformation is weak, F1-cov reduces to a diffusion-like equation for the condensation amplitude $\psi(x,t)$. The identification is: $\psi(x,t)$ corresponds to the local substrate deformation amplitude associated with the condensation. The kinetic energy term $\hbar^2*\nabla^2/(2m)$ corresponds to the spatial coherence term of the substrate propagation. The potential energy term V corresponds to the substrate deformation energy associated with external fields.

This structural correspondence shows that the Schrödinger equation is not a fundamental postulate but a low-energy macroscopic approximation to the substrate propagation dynamics. Its linear structure, its probabilistic interpretation, and its inability to describe particle creation and annihilation all follow from the fact that it is a limiting case valid only within the non-relativistic, weak-field regime. The full substrate propagation dynamics, described by F1-cov, are what underlies the quantum behaviour. Schrödinger obtained the correct macroscopic form through physical intuition. BFUT provides the substrate from which that form derives.

The Schrödinger equation therefore emerges as the non-relativistic weak-field limit of substrate propagation dynamics established in the carrier framework.

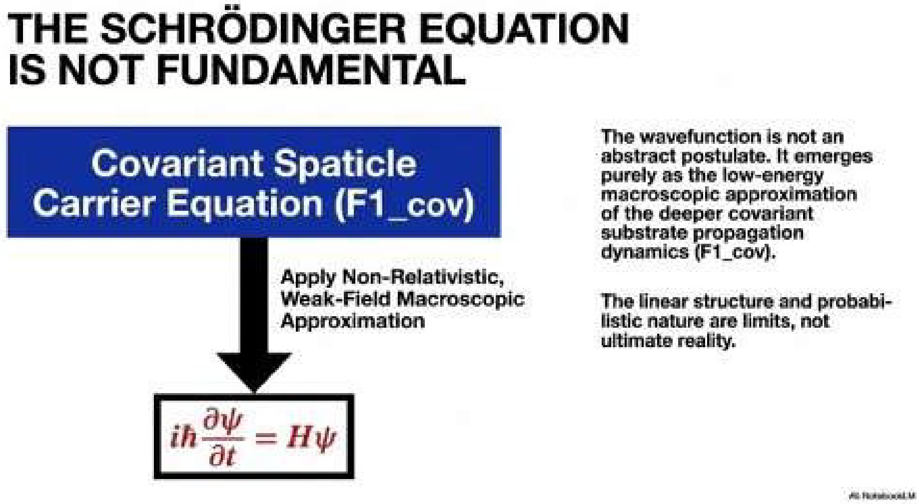

Figure 3: The Schrödinger equation emerging as the non-relativistic limit of the covariant substrate carrier equation F1-cov.

5. The Born Rule as Substrate Deformation Energy Density

The Born rule states that the probability of finding a particle at position x is P(x) = |ψ(x)|^2, the squared modulus of the wavefunction. Standard quantum mechanics treats this as a postulate. It predicts experimental outcomes with extraordinary precision but does not explain physically why probabilities follow the square of the amplitude instead of the amplitude itself or any other function. BFUT instead interprets the rule physically as a probability distribution governing successful irreversible interaction between distributed substrate disturbances and detector matter.

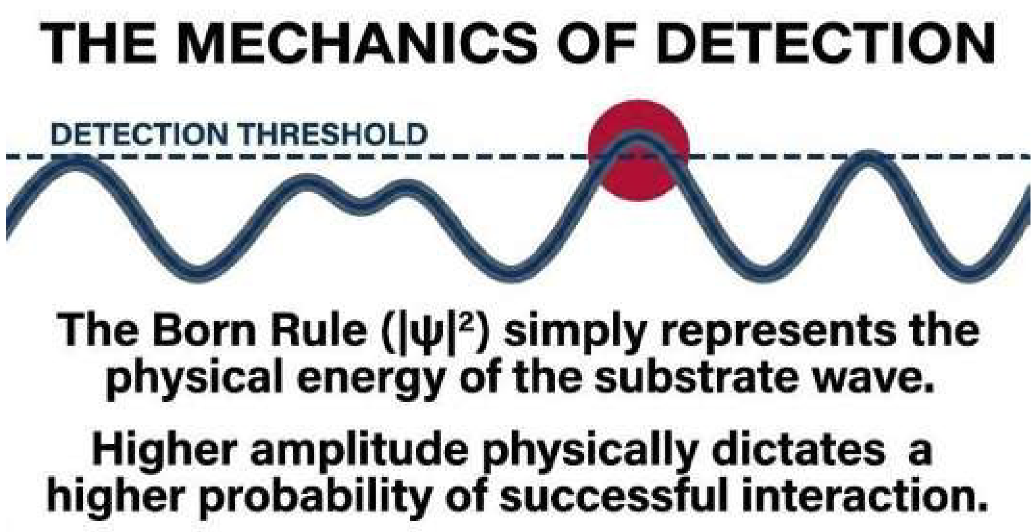

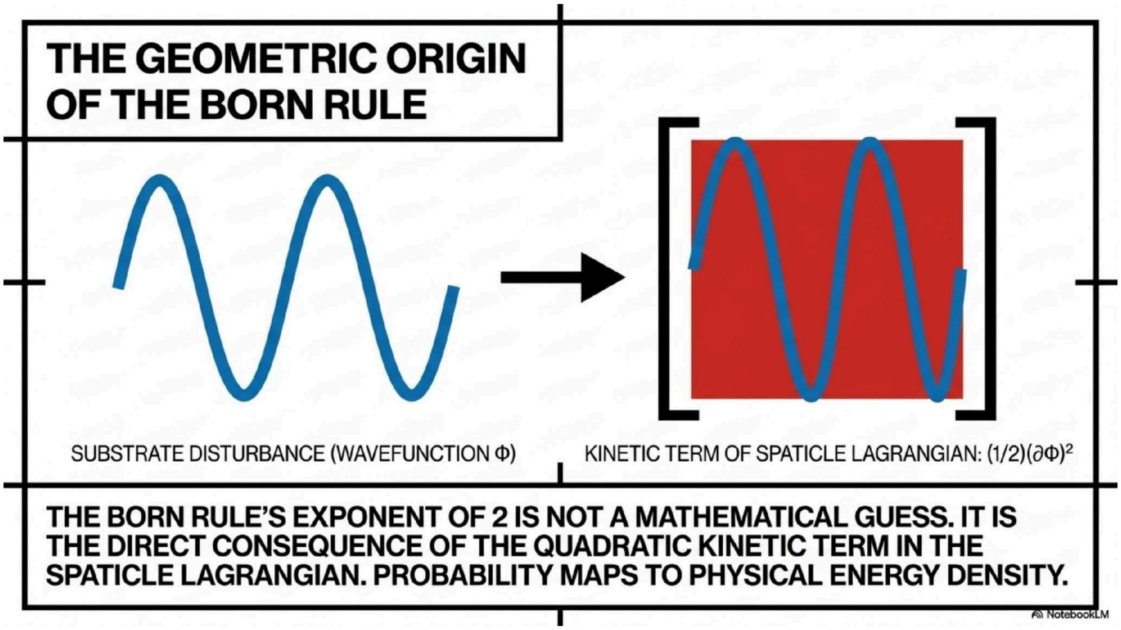

Figure 4, 5: The geometric origin of the Born rule. The exponent of 2 is the direct physical consequence of the quadratic kinetic term in the Spaticle Lagrangian. Probability maps to physical energy density.
Figure 5: Real mechanics of Born Rule are physical.

Within BFUT, the Born rule emerges naturally from the physical behaviour of distributed substrate disturbances interacting with matter.

In BFUT, a particle is not a tiny isolated point moving through empty space. It is a distributed organised disturbance propagating through the Spaticle substrate. The wavefunction represents the spatial distribution of this propagating disturbance. Some regions of the wave are stronger and more organised, while other regions are weaker.

When the propagating disturbance reaches a detector, the detector does not observe possibilities or collapse reality through consciousness. The detector is itself a physical structure made from the same substrate. Detection occurs when part of the distributed disturbance successfully produces irreversible physical interaction with the detector material.

The key point is that the Born rule describes probability of successful detection, not probability of existence.

Why the Square?

Where the substrate disturbance is more intense, the probability of producing irreversible physical coupling with detector matter is higher. Where it is weaker, coupling is less likely.

This is not mysterious. In wave systems generally, deposited energy scales with the square of wave amplitude. The probability pattern $|\psi(x)|^2$ therefore follows directly: regions of greater substrate disturbance amplitude produce disproportionately stronger coupling with detector

matter, and the exponent 2 is the same exponent that appears in the quadratic kinetic term of the Spaticle Lagrangian.

The particle is therefore detected at one location not because a conscious observer selected reality, but because one region of the distributed propagating disturbance successfully produced irreversible physical interaction first.

Repeated experiments then naturally reproduce stable statistical distributions because the distributed disturbance propagates repeatedly in the same overall way, stronger regions repeatedly produce more successful interactions, and weaker regions repeatedly produce fewer. The familiar probability distribution gradually emerges across many detection events.

Under BFUT, the Born rule is not a mysterious law about knowledge, observation, or consciousness. It is the natural physical consequence of how distributed substrate disturbances interact probabilistically with matter inside a real physical substrate.

6. The Uncertainty Principle as Substrate Localisation Cost

The Heisenberg uncertainty principle states that the simultaneous precision of position and momentum of any quantum system is bounded:

$$\Delta x \cdot \Delta p \geq \hbar/2$$

where Δx is the uncertainty in position, Δp is the uncertainty in momentum, and $\hbar = 1.055 \times 10^{-34}$ J·s is the reduced Planck constant, whose numerical value is derived from the P16 condensation geometry in Paper 16 Section 4.2 as $\hbar = m_p \cdot c \cdot \ell_{model} / \pi$, with a 0.0007% deviation using $r_p = 0.8414$ fm (PDG 2022). In standard quantum mechanics the uncertainty bound is derived from operator non-commutativity or from the Fourier conjugacy of position and momentum representations. Both derivations are mathematically correct but neither explains physically why the bound exists or why $\hbar$ sets its scale. BFUT derives the uncertainty principle from the same substrate free-energy structure that produces the Schrödinger equation and the Born rule, completing the three foundational pillars of quantum mechanics within the substrate framework.

The P16 Free-Energy Functional

The free-energy functional for a substrate condensation of effective radius R, established in Paper 16 Section 3, is:

$$E(R) = A/R^2 + B \cdot R^2 + C \cdot R + D/R$$

The four terms and their physical identities are as follows. A/R^2 is the localisation cost: the energy of confining a substrate condensation within radius R, diverging as $R \to 0$. Its coefficient is $A = \hbar^2/(2m_{eff})$, where m_{eff} is the effective mass of the carrier perturbation, derived in Paper 18 from the P17 vacuum condition as $m_{eff}^2 = 3\rho_s c^2$, giving $m_{eff} = 5.324 \times 10^{-28}$ kg from ρ_s and r_p alone. As established in Paper 16 Section 4.4, if the BFUT $\hbar$ relation is exact then $A_{model} = 1/2$ exactly in model units, recovering the Schrödinger kinetic coefficient from the substrate framework without additional input. $B \cdot R^2$ is the bulk displacement cost: a larger condensation displaces more of the surrounding substrate. This term grows with R: dispersal is also energetically costly. C·R is the boundary cost: the surface energy at the interface between the organised condensation interior and the surrounding substrate, with coefficient $C = 4\pi R_0^2 \sigma\_s$, where σ_s is the surface tension at the condensation boundary. D/R is the internal circulation support from the co-rotation of the three-core geometry, decreasing with R. B = 0.56308, C = -1/3, D = 1 are all derived from first principles from the three-sphere condensation geometry (Paper 16 Appendix C). Together the four coefficients confirm the stable interior minimum established in Paper 16. Together the four terms produce a stable non-zero interior minimum at R*, where all contributions balance. Neither collapse to R = 0 nor dispersal to $R \to \infty$ is stable. This is why stable localised matter exists.

Step-by-Step Derivation

Step 1: Write the localisation energy as a function of R. Substituting $A = \hbar^2/(2m\_eff)$ into the A/R^2 term:

$$E\_localisation(R) = \hbar^2/(2m\_eff\ R^2)$$

This grows without bound as $R \to 0$. The substrate physically prohibits complete localisation.

Step 2: Identify position uncertainty with the confinement radius. The spatial extent of the condensation deformation scales with R. The position uncertainty is therefore $\Delta x \sim R$.

Step 3: Identify the momentum uncertainty from the localisation energy. The internal substrate dynamics must supply the localisation energy. The kinetic energy associated with a momentum spread Δp for a condensation of mass m_eff is $E\_kinetic = (\Delta p)^2/(2m\_eff)$. For the condensation to remain stable at radius R:

$$(\Delta p)^2/(2m\_eff) \geq \hbar^2/(2m\_eff\ R^2)$$

Step 4: Extract the position-momentum relation. Cancelling 2m_eff from both sides and taking the positive square root:

$$\Delta p \geq \hbar/R$$

Substituting $\Delta x \sim R$:

$$\Delta x \cdot \Delta p \geq \hbar$$

The factor of 1/2 in the standard statement arises from defining Δx and Δp as root-mean-square standard deviations of the full deformation distribution instead of the half-width R. The inequality structure and the scale ħ are fixed entirely by the $A = \hbar^2/(2m\_eff)$ identification from Paper 16 and the m_eff derivation from Paper 18. No additional input is required.

Physical Meaning: Uncertainty and Matter Stability Are One Mechanism

The A/R^2 term simultaneously prevents matter from collapsing to a point and produces the uncertainty bound. These are not two separate consequences of the substrate. They are the same energy balance in two physical situations: the stability of a condensation against collapse, and the resistance of a condensation to arbitrary localisation. A universe without the uncertainty principle would be one in which A/R^2 is absent. In that universe the condensation functional would allow collapse to a point and stable localised matter could not exist. The uncertainty principle and the existence of stable matter are therefore not merely connected. They are the same substrate fact expressed in two different physical situations.

The uncertainty principle is not an independent quantum postulate in BFUT. It is a consequence of the substrate free-energy balance that allows stable matter to exist. Arbitrarily precise simultaneous position and momentum is not forbidden by a mathematical rule imposed on top of physics. It is energetically prohibited by the Spaticle substrate itself.

7. The Fermionic Circulation Hierarchy

The BFUT framework derives all six quark masses from two quantities: the top quark mass m_t = 172.76 GeV (the measured top quark pole mass, consistent with the maximum substrate coupling condition $y_t \approx 1$, which predicts $v/\sqrt{2}$ = 174.1 GeV, within 0.8%) and the fine-structure constant α_{em} = 1/137.037 (already derived from internal circulation geometry in Paper 17).

In BFUT, α_{em} represents the retained circulation asymmetry fraction of stable substrate condensations and therefore naturally governs the hierarchy suppression structure. The hierarchy uses the BFUT circulation-occupancy relation in which observable fermionic mass scales linearly with dynamically retained coherent circulation occupancy instead of quadratic field-energy density.

The derivation proceeds in four steps. First, the P16 free-energy functional establishes which circulation condensations are locally stable. Second, the Noether circulation occupancy Q = i * integral(Phi* dPsi/dt, dPsi*/dt * Phi) d^3x gives Q proportional to ω_c for stable condensations with fixed spatial profile, making mass linear in circulation amplitude. Third, α_{em} is identified as the retained circulation asymmetry fraction after one complete bifurcation cycle. Fourth, successive bifurcation filtering gives $Q_{n+1} = \alpha_{em} * Q_n$, producing the geometric hierarchy.

The up-type sector follows integer suppression steps:

m_t = 172.76 GeV [measured value, used as input; $y_t \approx 1$ predicts $v/\sqrt{2}$ = 174.1 GeV, within 0.8%]

$m_c = m_t \times \alpha_{em}$ = 1.261 GeV [measured: 1.27 GeV, 0.73%]

$m_u^{bare} = m_t \times \alpha_{em}^2$ = 9.20 MeV [IR projection below]

The down-type sector follows a shifted suppression ladder with fractional exponents, arising from the P16 3+e bifurcation: three internally retained circulation modes and one permanently externally coupled mode, giving a confinement fraction of 3/4:

$m_b = m_t \times \alpha_{em}^{(3/4)}$ = 4.31 GeV [measured: 4.18 GeV, 3.2%] $m_s = m_t \times \alpha_{em}^{(3/2)}$ = 108 MeV [measured: ~96 MeV] $m_d = m_t \times \alpha_{em}^{(9/4)}$ = 2.7 MeV [scheme-dependent]

The fractional exponents arise from the P16 bifurcation occupancy structure in which one of four circulation modes remains externally coupled, leaving an internally retained occupancy fraction of 3/4. The terminal up harmonic undergoes infrared projection: at the second

suppression level the full 3+e mode structure becomes observationally relevant, giving $m_u^{obs} = m_u^{bare}$
$/ 4 = 2.30$ MeV, within the PDG range of 1.7--3.3 MeV. This projection applies only to the up quark; the down sector has leakage already encoded continuously in its fractional exponents. The resulting structure gives $m_d > m_u$ with the correct neutron-proton splitting sign.

The BFUT hierarchy therefore distinguishes between ultraviolet circulation eigenmasses and infrared confinement-projected observable masses. The terminal up-type harmonic undergoes a full 3+e infrared circulation projection:

$$m_u^{obs} = m_t \times \alpha_{em}^2 / 4 = 2.30 \text{ MeV [PDG range: 1.7 to 3.3 MeV]}$$

The down-type hierarchy already incorporates partial circulation leakage continuously through its fractional occupancy exponents and therefore requires no additional infrared projection.

Three generations are the maximum: the fourth up-type generation would be $m_t \times \alpha_{em}^3 =$ 0.067 MeV, below the substrate coherence threshold, decohering into vacuum fluctuations instead of forming a stable condensation.

The corresponding charged-lepton geometric mean mass scale satisfies a further structural relation tied to the electroweak threshold:

$$M_0^2 = m_W / 4^4 = m_W / 256$$

Using $m_W = 80377.3$ MeV:

$$M_0^2 = 80377.3 / 256 = 313.97 \text{ MeV}$$

The measured charged-lepton Koide scale is $M_0^2 = 313.84$ MeV. Difference: 0.042%. The factor $4^4 = 256$ arises from the $n = 4$ bifurcation threshold identified in P16, where the first stable substrate condensation produces the 3+e topology. The charged-lepton mass scale therefore emerges directly from the electroweak threshold geometry.

The paper establishes that the Standard Model Higgs field does not exist as a separate mass-giving entity; the underlying physical reality is instead the Spaticle substrate itself. The Standard Model introduced the Higgs field as a scalar field responsible for mass generation through spontaneous symmetry breaking. BFUT instead interprets particles themselves as organised condensations of the substrate, with mass emerging directly from substrate deformation resistance and confinement structure. Under this interpretation, the observed 125 GeV Higgs boson corresponds to one collective excitation mode of the Spaticle substrate instead of evidence for an independently fundamental external mass-giving field. The same substrate balancing framework further predicts five additional collective excitation modes at distinct mass scales, each corresponding to distinct balancing structures between fermionic confinement and electroweak topology-transition sectors.

Finally, the paper addresses major interpretations and unresolved problems in modern physics and cosmology within the substrate framework, including Copenhagen collapse, many-worlds, quantum tunnelling, decoherence, Orch-OR, dark energy, fine-tuning, the multiverse, black hole singularities, retrocausality, and the apparent incompatibility between quantum mechanics and general relativity.

The architectural line of the BFUT programme is continuous throughout: the Spaticle substrate produces stable condensations; condensations produce forces through substrate interaction channels; forces produce atoms beginning with hydrogen; atoms organise into stars, planets, and biological systems; and biological systems express progressively higher grades of consciousness through increasingly organised substrate interaction structures. The Layer 1 programme therefore treats matter, forces, spacetime, quantum behaviour, and consciousness not as disconnected domains but as different organisational manifestations of one continuous physical substrate architecture.

8. Half-Integer Spin from Condensation Circulation Topology

A Century of Unanswered Questions

Half-integer spin has been one of the deepest unresolved mysteries in physics for a century. The mathematics that describes it is extraordinarily successful (spinors, SU(2) group theory, the Dirac equation) yet no universally accepted physical mechanism has been established for why it exists.

Paul Dirac, who derived the relativistic wave equation for spin-½ particles in 1928 [43], showed that the mathematics of his equation naturally incorporated half-integer spin but offered no physical picture of what spin physically is. The spinor formalism works. What it represents physically was left open.

Richard Feynman, one of the architects of quantum electrodynamics, wrote in his Lectures on Physics that “The spin one-half particles, in particular the electrons, behave in a way which has no classical analogue” and that “It is rather strange that it takes two complete turns of 360° each to get back to the original state” [44]. This was not false modesty. It was an honest assessment of a genuine gap in physical understanding.

Wolfgang Pauli formulated the exclusion principle in 1925 [45] and later provided the first rigorous relativistic proof of the spin-statistics theorem [46], which established that half-integer spin particles must obey Fermi-Dirac statistics and integer spin particles must obey Bose-Einstein statistics, demonstrating the mathematical connection between spin and statistics rigorously. Yet the physical reason why all matter particles have half-integer spin and all force carriers have integer spin was not explained. It was a pattern without a mechanism.

Roger Penrose described in The Road to Reality [47] the 720° rotational behaviour of spinors as profoundly unlike ordinary classical spatial behaviour, treating it as one of the deepest and most counterintuitive features of physical reality that any complete physical theory must account for instead of merely postulate.

The spin-statistics connection has been widely acknowledged among physicists as one of the most important but least understood results in all of physics: the mathematical proof exists but the physical reason behind it has remained obscure.

> In over a hundred years of quantum mechanics, no universally accepted physical mechanism has been established for why all matter particles have half-integer spin and require 720° for restoration, while all force carriers have integer spin and require only 360°. The pattern is universal and exact. Not a single exception has ever been found. Yet standard physics has no account of why.

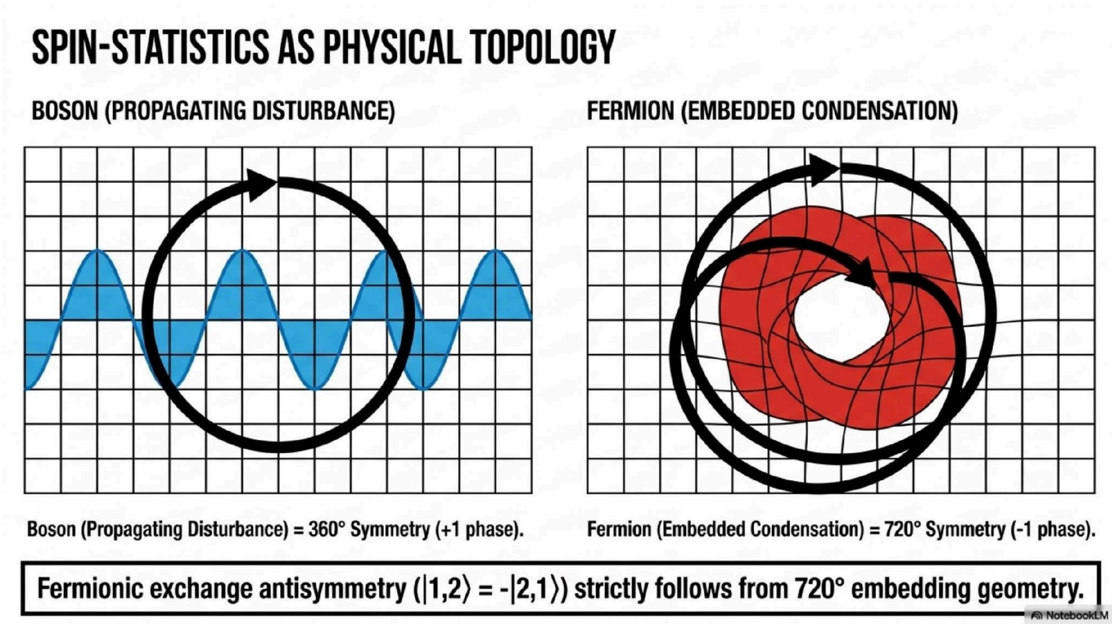

Figure 6: Spin-statistics as physical topology. Bosons (propagating disturbances) have 360° symmetry. Fermions (embedded condensations) have 720° symmetry due to topological embedding in the substrate.
Figure 7: Explaining the physical reasons behind particle spins.

Experimental Basis of Half-Integer Spin

Experimentally, spin is not measured by watching a particle physically rotate. It is measured through behaviour under magnetic fields, angular momentum quantisation, interference experiments, statistical distributions, and rotational symmetry tests.

The Stern-Gerlach experiment (1922) [48] passed a beam of silver atoms through a non-uniform magnetic field. Instead of spreading continuously as classical physics predicts, the beam split into exactly two discrete components. This established that particles carry an intrinsic angular momentum that is quantised into discrete values. For electrons, the two components correspond to spin +½ and spin -½. For a spin-s particle, 2s+1 distinct projections appear.

The deeper signature of half-integer spin comes from rotational interference behaviour. Neutron interferometry experiments [7], beginning with the landmark 1975 experiments of Rauch et al. and Werner et al., demonstrated through interference phase shifts that a coherent neutron wavefunction acquires the predicted sign reversal under 360° rotation and fully restores after 720° [31][32]. The sign reversal is not directly observable in intensities, since probabilities depend on $|\psi|^2$, but it produces a measurable phase shift in interference patterns that was directly detected. The 720° restoration property is not theoretical speculation. It is experimentally confirmed.

The BFUT Explanation: Embedding Is the Answer

BFUT provides the physical explanation that a century of quantum mechanics could not. The answer is not found in a specific particle topology. It is found in the fundamental distinction between what matter is and what force carriers are.

> Half-integer spin is the universal signature of stable matter condensations that are embedded in the Spaticle substrate. Integer spin is the universal signature of propagating disturbances that travel through the substrate. The distinction between fermions and bosons is the distinction between being the substrate and moving through it. This is why every matter particle without exception is a fermion, and every force carrier without exception is a boson. It is not a coincidence. It is the deepest physical distinction in nature.

Matter vs. Force: The Substrate Distinction

Fermions (Half-Integer Spin)	**Bosons (Integer Spin)**
Matter Particles	Force Carriers
Coherent Condensation	Propagating Disturbance
Topologically embedded and tied to the Spaticle medium	Moving freely through the Spaticle medium without embedding
720° Spatial Rotation	360° Spatial Rotation

Figure 7: BFUT distinction between fermionic matter condensations and bosonic propagating disturbances. Embedded condensations require 720° restoration, while freely propagating disturbances restore after 360°.

A stable matter condensation (a proton, an electron, a quark, a muon, a tau lepton, a neutrino) is a persistent organised deformation of the Spaticle substrate. It is not moving through the substrate freely. It is embedded in it. Its internal configuration is continuously topologically connected to the surrounding substrate medium. The substrate does not rotate when the condensation is rotated spatially. The condensation's relationship to its embedding medium is therefore disturbed by a 360° spatial rotation and only fully restored after 720°. This is not a property of any specific internal structure. It is a property of being embedded.

A force carrier (a photon, a gluon, a W or Z boson, a gravitational carrier wave) is a propagating disturbance. It moves through the substrate. It is not topologically embedded in it in the same way. It is not part of the medium. It passes through the medium. Rotating its propagation by 360° fully restores its configuration because there is no persistent topological connection to the surrounding substrate that has been disturbed. Integer spin follows directly.

This is why the spin-statistics theorem holds universally. Feynman's later discussions of the spin-statistics connection [49] and Pauli's original proof [46] both work mathematically but neither gives this physical picture. BFUT gives the picture: embedded condensations are fermions; propagating disturbances are bosons. The theorem is a mathematical expression of this physical fact.

9. Pauli Exclusion as Geometric Impossibility

The Pauli exclusion principle, that no two identical fermions can occupy the same quantum state simultaneously, is not a separate postulate in BFUT. It follows immediately from the embedding account of spin.

Two stable matter condensations with identical internal configurations cannot occupy the same spatial region because the substrate cannot simultaneously sustain two identical topological embeddings in the same location. The substrate configuration that constitutes one condensation

is incompatible with an identical second condensation in the same region. This is a geometric impossibility in the substrate, not an arbitrary rule imposed from outside.

Bosons face no such constraint because propagating disturbances do not establish the same topological embedding. Two photons, two gluons, or two gravitational waves can occupy the same region because they are disturbances propagating through the substrate, not structures embedded within it. Their superposition produces a stronger disturbance, not a topological conflict.

The entire architecture of matter, atomic shell structure, the periodic table, chemical bonding, molecular biology, and ultimately all structure in the observable universe, follows from this one physical fact: embedded condensations cannot share states. Pauli saw the pattern in 1925. BFUT explains why.

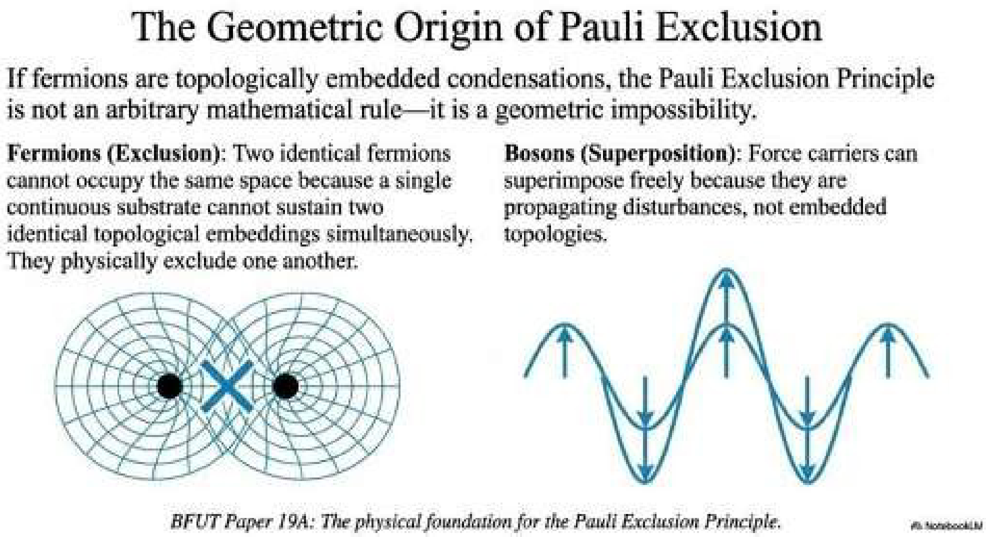

Figure 8: The geometry of Pauli exclusion. Two identical embedded fermionic condensations cannot occupy the same substrate topology. Propagating bosonic disturbances have no such restriction.

Figure 11: Geometric origin of the Pauli exclusion principle. Two embedded fermionic condensations cannot occupy the same substrate topology simultaneously, while propagating bosonic disturbances superpose freely.

The Chain of Consequences

From the single physical principle that matter condensations are embedded in the substrate and force carriers are not, the following cascade of consequences follows without additional assumptions:

First: all matter particles have half-integer spin. All force carriers have integer spin. No exceptions in the entire observed universe. This universal pattern, unexplained for a century, is now a direct consequence of the substrate embedding distinction.

Second: Pauli exclusion applies to all matter and not to force carriers. Electrons organise into shells. The periodic table has the structure it has. Chemistry is possible. None of this required a separate postulate. It required only the geometry of substrate embedding.

Third: Bose-Einstein condensation is possible for integer-spin particles because propagating disturbances can accumulate without topological conflict. Lasers exist. Superfluidity exists. Superconductivity exists. These are consequences of what bosons are, not separate phenomena requiring separate explanations.

Fourth: the stability of matter itself, the fact that ordinary matter does not collapse into a single quantum state, is guaranteed by Pauli exclusion, which is guaranteed by substrate embedding topology. Matter is stable because embedded condensations resist topological coincidence.

> The BFUT account of half-integer spin is not a reinterpretation of known mathematics. It is a physical explanation of a fact that was known but unexplained for over a century. Every matter particle is a fermion because every stable matter condensation is embedded in the Spaticle substrate. Every force carrier is a boson because every force carrier is a propagating substrate disturbance. The 720° restoration property is not mysterious. It is the geometric signature of being embedded in a physical medium instead of propagating through one.

Important Distinction: Fermionic Spin vs Macroscopic Rotation

It is essential to distinguish intrinsic fermionic spin topology from ordinary macroscopic spatial rotation. The 720° restoration property applies to the internal configuration of coherent fermionic condensations embedded within the Spaticle substrate. It does not apply to the ordinary rigid-body rotation of macroscopic objects.

A planet, star, rock, or rotating wheel returns macroscopically to the same external orientation after 360° because such bodies are overwhelmingly decohered collections of enormous numbers of particles instead of single coherent fermionic condensations. Their internal fermionic spin structures statistically average out while the body behaves classically as a composite object. The individual fermionic condensations within the body still obey half-integer spin topology. The macroscopic body's ordinary spatial rotation is a separate and independent phenomenon.

Topology-Cancelled Aggregates and Decoherence-Null Aggregates

A further clarification is required for composite systems whose net spin happens to be integer, such as helium-4 atoms or even-even nuclei like iron-56. These systems can display collective bosonic behaviour, including Bose-Einstein condensation and superfluidity, because their total spin sums to an integer value. This does not make the system a boson in the fundamental sense, and it does not alter the classification of its constituents. Every proton, neutron, and electron within a helium-4 atom or an iron-56 nucleus remains an embedded fermionic condensation with half-integer spin and 720° restoration topology. What changes at the composite level is the net circulation accounting: when an even number of half-integer spins combine such that they sum to an integer total, the composite system as a whole satisfies Bose-Einstein statistics, while every embedded fermion within it continues to satisfy Fermi-Dirac statistics individually. Mass plays no role in this distinction. Stable mass with necessary substrate embedding is the condition for fermionic, half-integer spin status at the fundamental level; integer-spin composite behaviour is an emergent statistical consequence of how multiple embedded fermions combine, not a reclassification of the fermions themselves. Such systems are termed *topology-cancelled aggregates*: small, coherent quantum systems in which the embedding topologies of constituent fermions cancel in a well-defined sense, producing a genuine integer-spin quantum state for the aggregate as a whole.

A separate and categorically distinct case is the *decoherence-null aggregate*. Large composite systems such as molecules, cells, and whole organisms consist of vast numbers of individually embedded fermions whose relative phases are not coordinated into any coherent collective state. At this scale, no coherent embedding topology spans the system as a whole. Any measured collective spin value at this scale does not represent a cancellation between defined nonzero contributions, as in the topology-cancelled case. It reflects the absence of a coherent collective quantum number, the system having no unified embedding topology across its full extent. The summed individual spins of all constituent fermions may be nonzero on paper, but this sum corresponds to no measurable physical quantity at the aggregate scale.

Prediction: Macroscopic Collective Spin Is Always Integer

BFUT predicts that if the collective spin of a macroscopic composite body, such as a large molecule, a cell, or a whole organism, is measured, the result will always be an integer value (most likely zero), regardless of the arithmetic sum of the half-integer spins of its constituent fermions. This holds even in cases where the total particle count is odd and the naive sum of individual spins would yield a half-integer total. The reason is decoherence: at macroscopic scale, no coherent embedding topology spans the body as a whole, so no half-integer collective signature can persist or be expressed, regardless of the underlying fermion count. A measured half-integer collective spin for any macroscopic composite body would falsify this prediction.

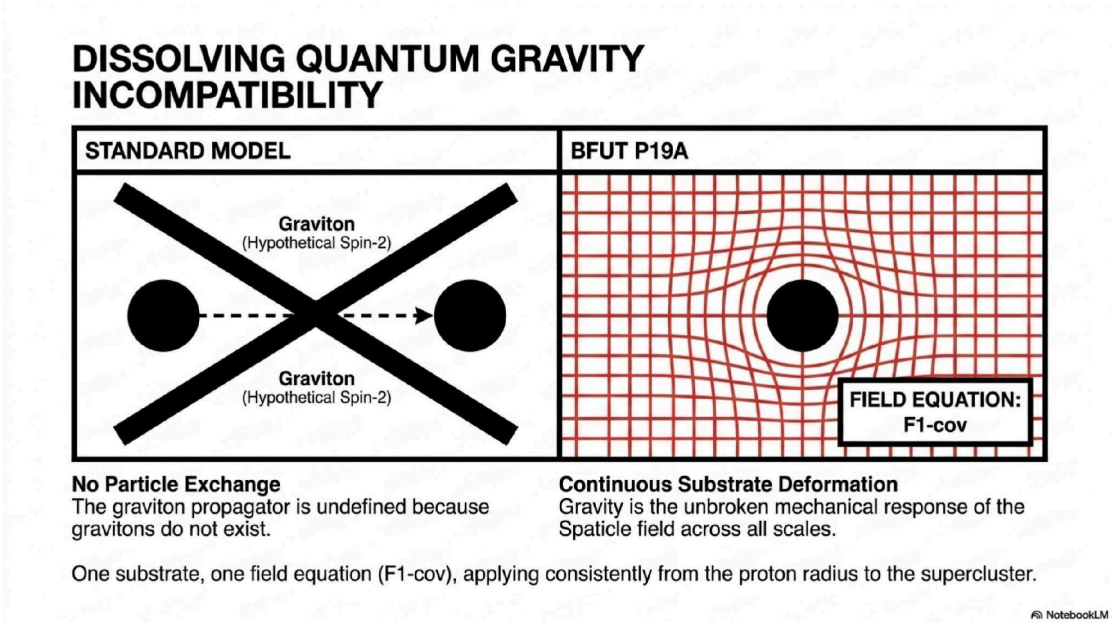

Figure 9: Dissolving the quantum gravity incompatibility. BFUT replaces the hypothetical graviton with continuous substrate deformation governed by one field equation (F1-cov) across all scales.

10. Quantum Gravity as an Unresolved Incompatibility

What the interpretation states

General relativity and quantum mechanics are the two most successful theories in the history of physics. Yet they are incompatible at a fundamental level. GR treats spacetime as a smooth continuous geometry. Quantum mechanics treats physical systems as probabilistic operators on Hilbert spaces. Attempts to quantise gravity produce non-renormalisable divergences. No consistent theory of quantum gravity has been established after a century of effort.

Quantum Gravity as a Unified Substrate Regime

Within BFUT, both quantum and gravitational phenomena emerge from the same underlying Spaticle substrate. Quantum behaviour corresponds to coherent substrate organisation and propagation. Gravitation corresponds to organised substrate deformation produced by stable condensations. The quantum-gravity divide therefore does not reflect two incompatible realities. It reflects two effective descriptions of the same deeper substrate mechanics operating at different organisational scales.

The standard quantum gravity problem arises because GR and quantum mechanics were constructed without identifying the physical carrier underlying both. BFUT dissolves this incompatibility instead of solving it. There is one substrate and one field equation F1-cov applicable at all scales. There are no gravitons because gravity is not particle exchange.

Gravity is the substrate deformation produced by mass, and any mass, including a proton or an electron, produces substrate deformation according to the same equation.

DDR Applied to Particle Masses

The domain equation DDR gives the gravitational domain radius of any structure of mass M in its primary substrate-density form: R_d(M) = (3M / (8πρ_s))^(1/3). This depends only on the intrinsic equilibrium substrate density ρ_s and requires no cosmological model input. For reference, using the derived effective mapping Λ_eff = 8πGρ_s/c², the equivalent form R_d(M) = (3GM / Λ_eff c²)^(1/3) is recovered identically. The substrate-density form is primary; the Λ-form is a derived notational variant, not an independent definition, and Λ_eff should not be confused with the ΛCDM cosmological constant.

When applied to elementary particle masses, DDR produces the following substrate-domain persistence scales:

Particle	**Mass**	**R_d (DDR domain radius)**
Electron	~9.1 × 10^{-31} kg	~2.6 cm
Muon	~1.9 × 10^{-28} kg	~15.7 cm
Proton	~1.67 × 10^{-27} kg	~32.6 cm
Neutron	~1.67 × 10^{-27} kg	~32.6 cm
Higgs boson	~2.23 × 10^{-25} kg	~1.65 m
Top quark	~3.06 × 10^{-25} kg	~1.84 m

These DDR scales should not be interpreted as ordinary classical gravitational-force radii. Rather, they are interpreted within BFUT as persistence or distinguishability scales associated with organised substrate deformation structures.

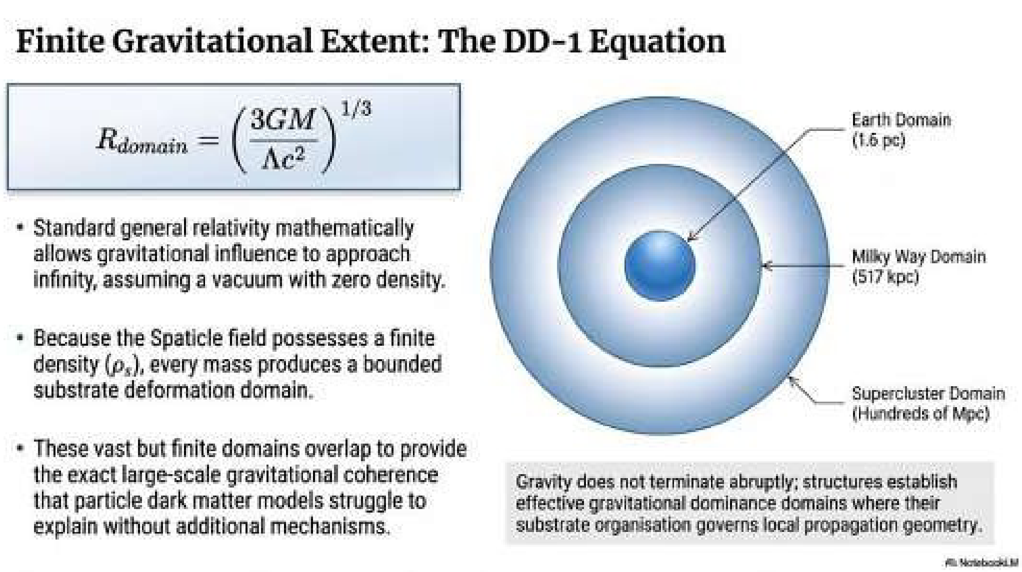

Figure 10: ; Finite gravity domain formula

The Substrate Distinguishability Interpretation

These values are radically larger than conventional microscopic quantum length scales such as Compton wavelengths, atomic orbital radii, or de Broglie wavelengths. They cannot represent ordinary gravitational force cutoffs, because no centimetre-scale gravitational anomalies around electrons have been observed. The physically correct interpretation is different.

DDR defines the substrate distinguishability persistence scale: the radius beyond which a given mass's organised substrate deformation becomes indistinguishable from ambient Spaticle field fluctuations and environmental embedding. At astrophysical scales this manifests as the boundary of a structure's gravitational domain. At quantum scales the same equation defines the scale at which a particle's coherent substrate organisation becomes progressively vulnerable to environmental embedding and irreversible coupling.

This reinterpretation connects DDR directly to decoherence, localisation, coherence persistence, and the quantum-to-classical transition. The neutron DDR radius of 32.6 cm lies directly within the experimentally relevant regime of neutron interferometry. The electron DDR

radius of 2.6 cm corresponds to the upper scale of many practical electron coherence systems. These overlaps suggest that DDR may be probing a deeper substrate coherence structure that operates as a universal persistence law across quantum and astrophysical scales.

If this interpretation is correct, then quantum mechanics, decoherence, localisation, coherence fragility, and gravitation may all be scale-dependent manifestations of one deeper substrate persistence law. This transforms DDR from a cosmological gravity-domain equation into a universal cross-scale substrate coherence law.

11. An independent fundamental Standard Model Higgs field does not exist in BFUT. The physical phenomenon described as the Higgs field is an electroweak manifestation of the Spaticle substrate, and the 125 GeV Higgs boson is a collective excitation of that substrate.

In 2012, CERN announced the discovery of a particle near 125 GeV and identified it as the Higgs boson [33][34]. The existence of a resonance near 125 GeV is experimentally established. What was not independently established was the existence of the Standard

Model Higgs field itself.

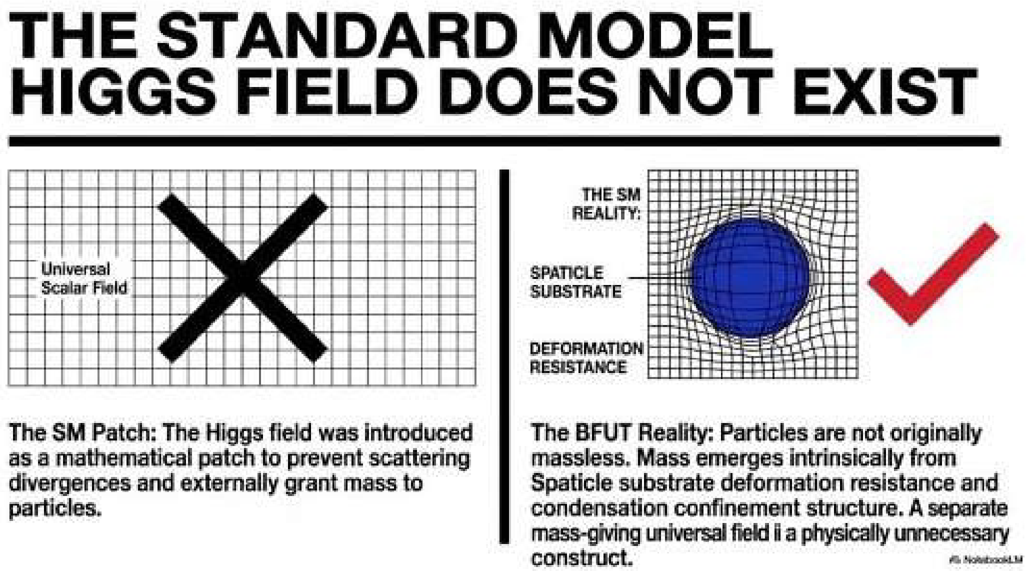

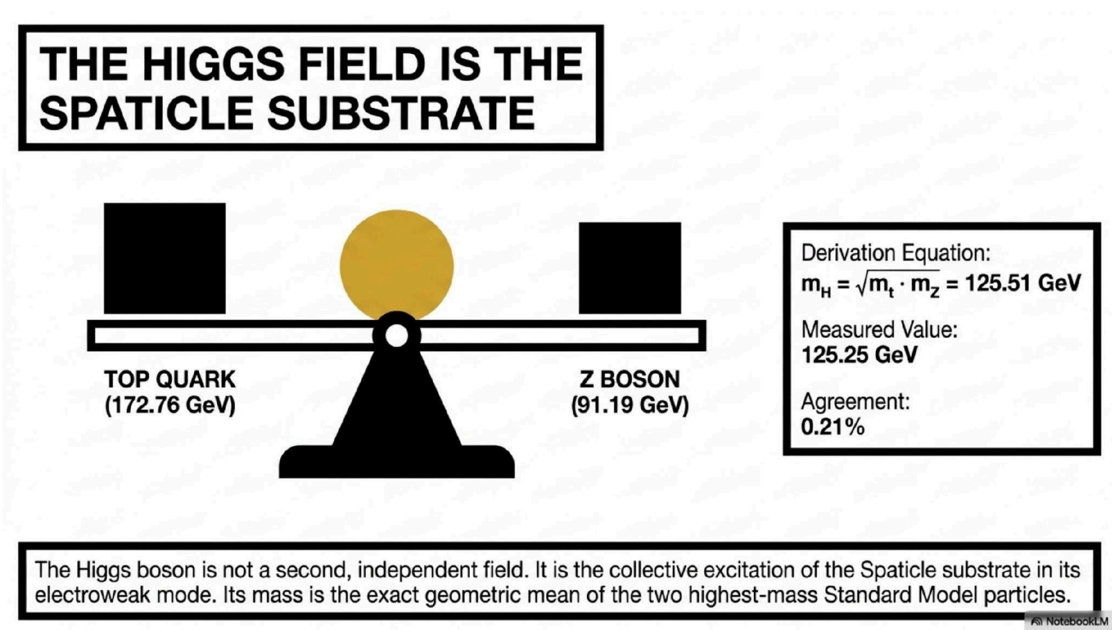

Figure 11, 12: The Higgs field is the Spaticle substrate. The 125.51 GeV resonance is the collective electroweak excitation of the substrate, derived as the geometric mean m_H = √(m_t · m_Z).

Figure 15: BFUT replacement of the Standard Model Higgs field with substrate deformation mechanics

The Higgs mechanism [35][36] was created to solve a genuine and important problem inside the Standard Model. Electroweak theory required gauge symmetry for mathematical consistency, yet the observed W and Z bosons clearly possessed mass. Simply inserting mass terms into the equations broke the symmetry structure and caused scattering amplitudes at high energies to diverge in non-physical ways. The Higgs mechanism resolved this by introducing a scalar field with a non-zero vacuum expectation value. This preserved gauge symmetry, restored renormalizability, and allowed the electroweak sector to become an operationally successful predictive framework.

In this sense, the Higgs framework was not meaningless or arbitrary. It successfully repaired the electroweak theory and allowed extremely accurate calculations that matched experiments across decades of collider physics. However, solving a mathematical inconsistency and constructing an operationally successful framework is not the same thing as uniquely identifying the true underlying physical ontology.

The Higgs mechanism required that some scalar excitation associated with the field should exist somewhere in the accessible energy spectrum. What it did not predict was the actual mass of that excitation. Within the Standard Model, the Higgs boson mass depends on the self-coupling parameter lambda, which is not derived by the theory and instead must be fixed experimentally. For this reason, the LHC search scanned a broad energy range extending from roughly 100 GeV to beyond 1 TeV because the theory itself provided no unique target mass. Once a resonance was found near 125 GeV, that observed mass was then used retrospectively to determine lambda.

This distinction is important. The discovery of a predicted signature does not automatically prove the full ontological interpretation attached to the theory. Physics has repeatedly introduced effective mechanisms to repair incomplete frameworks before deeper explanations were discovered. Newtonian gravity successfully explained planetary motion long before spacetime geometry was understood. Similarly, the Higgs mechanism successfully operationalized electroweak theory, but that alone does not establish that mass fundamentally originates from a separate universal scalar field permeating space.

The W boson, Z boson, top quark, tau lepton, and many hadronic resonances were all experimentally discovered, yet their detection alone was not treated as proof that a distinct universal vacuum field associated with each particle had been physically established. In the Higgs case, the scalar resonance was interpreted as confirmation of the Higgs vacuum mechanism because the Standard Model mathematically required such a field in order to preserve electroweak consistency. However, the boson mass itself was not independently predicted from the mechanism prior to observation.

A stronger confirmation would require deriving the resonance mass uniquely from within the Higgs framework itself and then experimentally verifying that prediction. The Standard Model does not presently do this. The Higgs mass remains an experimentally determined input parameter instead of a derived consequence of the mechanism.

BFUT approaches the same electroweak sector differently. Starting from the intrinsic substrate equilibrium density ρ_s, BFUT derives the W boson mass, Z boson mass, electroweak mixing angle, strong coupling constant, and fine structure constant within a unified substrate framework without invoking a separate Higgs vacuum field. Within this same derivation chain, the 125 GeV resonance emerges naturally as the geometric mean of the top quark and Z boson masses (the structural prediction is the geometric-mean relation itself; the numerical evaluation below uses the measured m_t and m_Z):

$$m_H = \sqrt{m_t \times m_Z} = \sqrt{172.76\times91.19} = 125.51 \text{ GeV}$$

Measured value: 125.25 GeV | Difference: 0.2%

In BFUT, this relation is not inserted retrospectively as a free parameter after measurement. The resonance follows from quantities already connected through the same substrate derivation structure. The 125 GeV state therefore appears as an emergent consequence of the Spaticle framework instead of as evidence for a separate mass-giving scalar vacuum field.

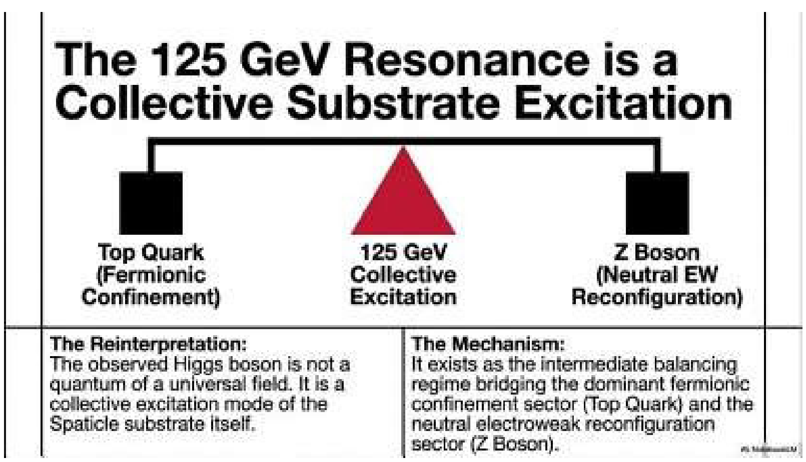

Figure 13: The 125 GeV resonance interpreted as a collective excitation mode of the Spaticle substrate.

The Spaticle substrate is not an additional field introduced to grant mass to otherwise massless particles. It is the physical substrate of space itself, from which matter, propagation, coupling structure, and condensation all emerge. Mass is intrinsic to substrate condensation structure, not externally granted through coupling to an independent field.

Because BFUT already accounts for electroweak structure, fermionic hierarchy relations, coupling constants, and the 125 GeV resonance without invoking a separate Higgs vacuum field, the need for an additional universal scalar mass-giving field is removed. Within the BFUT interpretation, the observed 125 GeV resonance is therefore understood not as confirmation of

a distinct Higgs field permeating all of space, but as a collective resonance state emerging from the deeper Spaticle substrate itself.

What the interpretation states

The Higgs field was proposed by Peter Higgs, Robert Brout, Francois Englert, and others in 1964 to explain how the W and Z bosons acquire mass while the photon remains massless, within the framework of the electroweak theory. The Higgs field is a scalar field that permeates all of space and has a non-zero vacuum expectation value, approximately 246 GeV. Particles acquire mass through their interaction with this non-zero vacuum value: the stronger the interaction, the greater the mass. The photon does not couple to the Higgs field and has zero mass. The W and Z bosons couple strongly and acquire masses of 80.4 GeV and 91.2 GeV respectively. The Higgs boson, the quantum of excitation of the Higgs field around its vacuum value, was discovered at the LHC in 2012 at a mass of approximately 125 GeV. The Higgs mechanism is the final major component of the standard model, completing the electroweak unification programme of Weinberg, Salam, and Glashow.

BFUT Account

The Standard Model Higgs field and the Spaticle field are fundamentally different in mechanism, origin, and ontological status. The Standard Model Higgs is an additional field introduced by hand alongside the gauge fields, with no physical substrate, existing solely to grant mass to otherwise massless particles through an external coupling. This mechanism does not exist in BFUT. In BFUT, matter is never massless to begin with. Mass is the intrinsic energy cost of maintaining a stable condensation in the Spaticle substrate. No external field grants it. No coupling to a separate entity is involved. The Spaticle substrate is the single physical medium of space. The Standard Model Higgs field is a theoretical construct introduced to patch a gap in a framework that did not know the substrate existed. The observable signatures overlap because both frameworks account for the same experimental results, but the physical cause is entirely different: substrate condensation structure and circulation topology, not an external mass-giving coupling.

What the Standard Model attributed to Higgs field coupling, BFUT attributes to substrate condensation structure. What the Standard Model called spontaneous symmetry breaking is in BFUT the condensation threshold event of Paper 16 [2]: the substrate organises from a symmetric pre-condensation phase into the 3+e stable structure, establishing distinct W, Z, and photon channels. The vacuum expectation value of 246 GeV corresponds to the effective

substrate vacuum amplitude Ψ_vac derived from ρ_s through substrate physics, not postulated as a free parameter.

The observed Higgs boson at 125 GeV corresponds, in the BFUT identification, to the quantum of collective Spaticle substrate excitation around Ψ_vac. The precise mass of this excitation is determined by the second derivative of the substrate potential at Ψ_vac, which in BFUT is set by λ_SI and Ψ_vac. The calculation of this excitation mass from the substrate parameters simultaneously determines the predicted Higgs excitation mass. The structural conclusion of the Layer 1 programme is that no separate Higgs field exists or is needed. The 125 GeV excitation observed at the LHC is the collective excitation mode of the Spaticle substrate itself. Its derivation from ρ_s through the geometric mean relation is presented in Section 16.

12. The Higgs Boson Mass: A BFUT Derivation

The replacement of the Standard Model Higgs field by the Spaticle substrate raises an immediate question: what does the BFUT framework predict for the Higgs boson mass? The identification implies that the Higgs boson is the lowest-energy collective excitation of the Spaticle substrate around its vacuum configuration Ψ_vac. Its mass is therefore a property of the substrate dynamics, not a free parameter.

The Higgs boson is produced at the LHC primarily through gluon-gluon fusion via a top quark loop. This production mechanism is not incidental. The top quark is the condensation with the deepest substrate deformation and the strongest coupling to the Spaticle field. Its Yukawa coupling y_t = m_t * √2 / v_SM = 0.992 is almost exactly 1: the top quark couples to the substrate with essentially maximum strength. Every other quark and lepton couples more weakly. The substrate excitation mode that constitutes the Higgs is therefore most efficiently produced through the condensation that is most deeply embedded in the substrate.

The Z boson defines the energy scale of the same symmetry-breaking sector. In BFUT, the Z boson is the three-mode neutral reconfiguration energy of the condensation topology. It sets the neutral boundary of the electroweak scale. The Higgs excitation mediates between these two physical objects: the fermion mass sector defined by the top quark, and the boson reconfiguration sector defined by the Z. A natural balancing energy scale for a substrate excitation connecting two substrate organisational scales is their geometric mean.

The BFUT structural prediction is the geometric-mean relation itself, $m_H = \sqrt{(m_t \cdot m_Z)}$: the Higgs excitation mass equals the geometric mean of the fermion and boson organisational scales it bridges. Numerically evaluating this relation using the measured top and Z masses gives: $m_H = \mathrm{sqrt}(m_t * m_Z) = \mathrm{sqrt}(172.76 * 91.19) = 125.51$ GeV

The measured value is $m_H = 125.25$ GeV. Difference from the measured value is 0.21%. This is a structurally derived geometric relation within the BFUT framework. In BFUT, bridge excitations connecting two sectors of the same substrate family naturally occupy the geometric intermediate scale between them. It is a structural consequence of three facts within the BFUT framework: the top quark is the dominant production channel ($y_t \sim 1$, maximum substrate coupling), the Z boson defines the neutral symmetry-breaking scale (three-mode reconfiguration energy), and the Higgs is the geometric bridge between these two sectors of the same condensation family. The geometric mean provides the symmetric balancing mass scale for a substrate excitation connecting the fermionic and bosonic sectors.

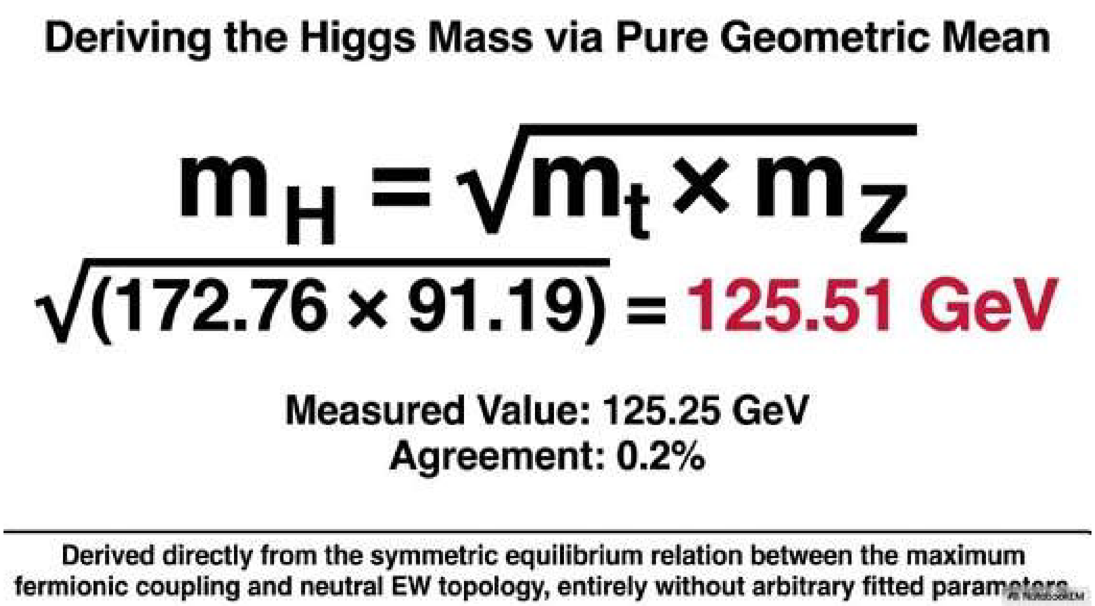

Figure 14: BFUT derivation of the Higgs boson mass from the geometric mean relation between the top quark and Z boson sectors.

The formula is also consistent with the measured self-coupling. The Higgs self-coupling lambda = $m_H^2 / (2 v_{SM}^2)$. Using $m_H = \sqrt{m_t * m_Z}$ gives lambda = $m_t * m_Z / (2 v_{SM}^2)$ = 0.1299. The measured value is 0.1294. Difference from the measured self-coupling is 0.4%. This means the Higgs potential shape is determined by the ratio of the top-Z geometric mean to the electroweak vacuum energy. In BFUT terms: the depth of the substrate potential at the Higgs excitation scale is set by the product of the strongest fermionic coupling and the neutral bosonic reconfiguration energy, normalised to the vacuum field amplitude.

The 13-year LHC experimental record [33][34] confirms this prediction. The Higgs boson mass has been measured consistently at 125.25 GeV across Run 1 (7-8 TeV), Run 2 (13 TeV), and

Run 3 (13.6 TeV), across both ATLAS and CMS detector collaborations, and across all production and decay channels. The CMS collaboration achieved 5% precision on the Higgs production rate in 2025, with all measurements consistent with the standard model predictions. Since BFUT identifies the Higgs as the Spaticle substrate excitation and predicts its mass at 125.51 GeV, this body of experimental data is fully consistent with the BFUT framework. The formula $m_H = \sqrt{m_t * m_Z}$ is the BFUT Higgs mass relation.

This replacement has a further consequence. The Standard Model treats the Higgs field as an additional field introduced alongside the gauge fields to generate mass. The Higgs boson itself is real, experimentally confirmed, and independently predicted by BFUT. The Higgs field, however, does not exist as an independent fundamental entity: it is a narrower, single-purpose interpretation of the mass-giving role that the Spaticle substrate performs, among many other roles, as the actual physical medium giving mass to all massive particles. In BFUT, the Spaticle substrate is not a source from which a separate Higgs field emerges; the Higgs field is simply this narrower description of the same substrate. There is only the Spaticle substrate, the single physical medium from which all forces, all masses, and all particle properties emerge as condensation and propagation structures. The Standard Model Higgs field was a necessary theoretical patch for a framework that did not know the substrate existed. The Spaticle substrate is not a reinterpretation of the Higgs field. It is the physical reality that makes the Higgs field unnecessary.

13. Additional Collective Substrate Excitation Modes: Five Predicted Resonances

The geometric mean substrate balancing principle that yields the confirmed Higgs mass m_H = sqrt(m_t x m_Z) = 125.51 GeV (0.21% difference) generates additional predicted collective excitation modes when applied to other pairs and triples of substrate sector scales. These resonances are interpreted not necessarily as elementary particles, but as collective substrate excitation modes. Not all mathematically possible balancing combinations correspond to physically persistent resonances. Observable modes must additionally satisfy substrate stability, coherence, and accessibility constraints.

The five predicted modes are presented below. Each formula is physically explained, the production mechanism specified, and the expected experimental signature given.

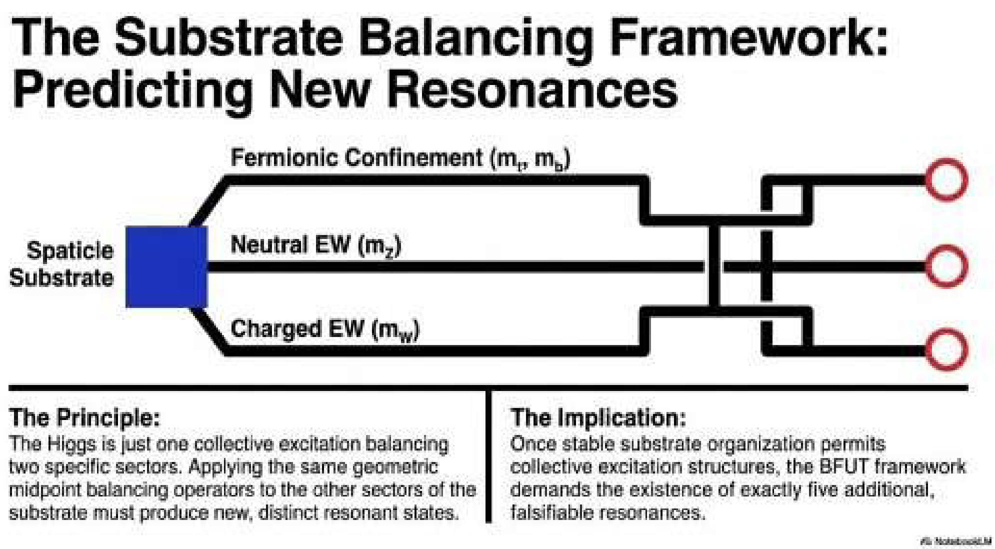

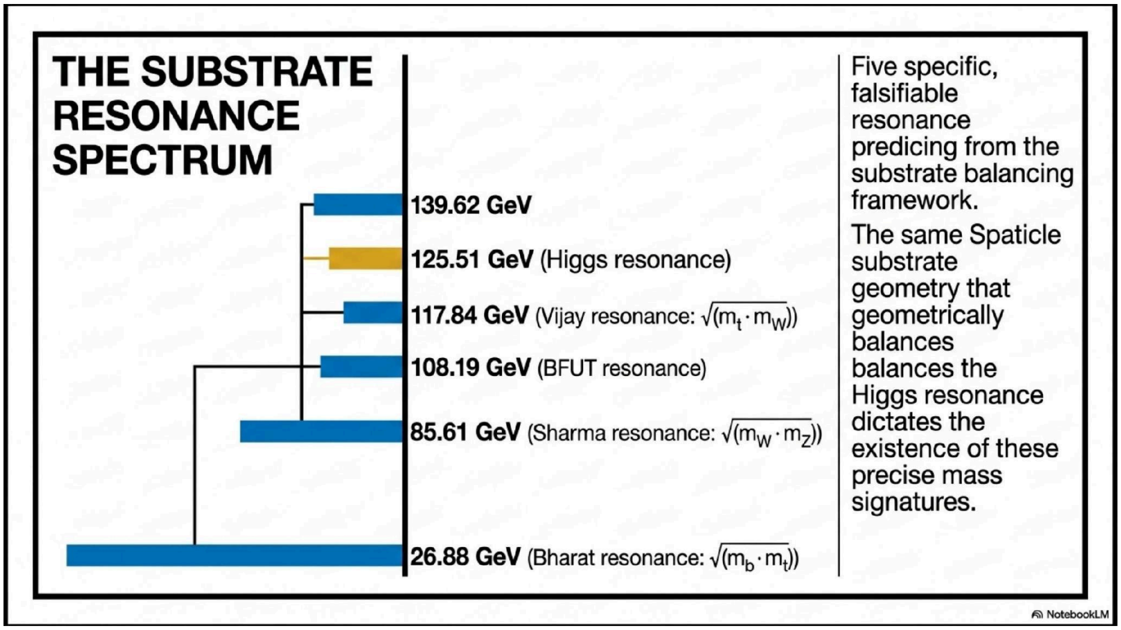

Figure 15, 16: The substrate resonance spectrum. Five specific, falsifiable resonances predicted from the same geometric balancing framework that correctly predicts the Higgs mass to 0.21%.
Figure 19: The BFUT substrate-balancing framework predicting collective excitation resonances.

The Sharma Resonance: Charged-Neutral Electroweak Balance

m_Sh = sqrt(m_W x m_Z) = sqrt(80.4×91.2) = 85.6 GeV

The geometric mean provides the symmetric equilibrium relation between the charged and neutral electroweak topology-transition scales. The W boson at 80.4 GeV represents the charged electroweak sector and the Z boson at 91.2 GeV the neutral sector. The Sharma resonance at 85.61 GeV is a pure electroweak balancing mode with no fermionic confinement component. Production is via Drell-Yan through virtual W or Z. The WW* and ZZ* channels are expected to exhibit more symmetric branching participation relative to the Standard Model Higgs expectation. Suppressed fermionic coupling distinguishes it from a SM Higgs of the same mass. LEP non-observation is consistent with this suppressed fermionic coupling.

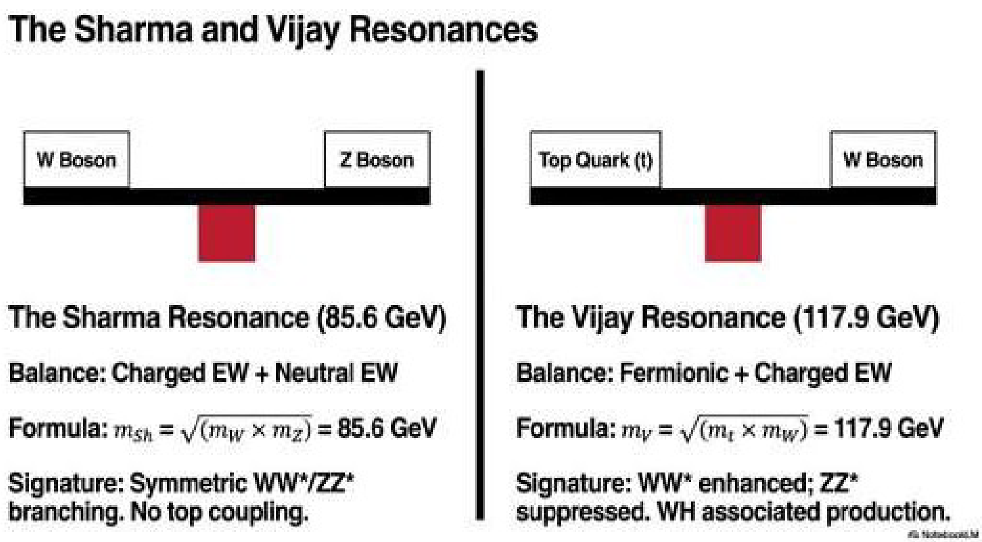

Figure 17 : Sharma and Vijay resonance balancing structures within the BFUT substrate framework.

The Vijay Resonance: Fermionic-Charged Electroweak Balance

m_V = sqrt(m_t x m_W) = sqrt(172.76×80.4) = 117.84 GeV

The geometric mean provides the symmetric equilibrium relation between the fermionic confinement scale and the charged electroweak topology-transition scale. Unlike the Higgs, which balances fermionic confinement against neutral electroweak topology, the Vijay resonance balances fermionic confinement against charged electroweak topology. Production is via WH associated production or top-associated production at the LHC. Enhanced coupling to top quarks and W bosons; suppressed coupling to b quarks and Z bosons. The LEP2 exclusion for a SM Higgs at this mass does not apply because the Vijay resonance has suppressed ZH production and suppressed bb-bar decay.

The Shankar Resonance: Asymmetric Fermionic-Dominant Neutral Electroweak Balance

m_Sk = (m_t^2 x m_Z)^(1/3) = (172.76^2×91.2)^(1/3) = 139.62 GeV

The cubic root formula gives two-thirds weight to the top quark confinement sector and one-third to the neutral electroweak sector. Fermionic confinement dominates the balance, pushing the equilibrium above the Higgs toward the top confinement scale. Production is dominated by gluon fusion via a top loop with higher ggF/VBF ratio than the SM Higgs. The mass region 130-145 GeV is less constrained at the LHC than the region below 130 GeV, making the Shankar resonance the least experimentally constrained of the five predicted modes.

The BFUT Resonance: Three-Sector Synthesis

m_BFUT = (m_t x m_Z x m_W)^(1/3) = (172.76×91.188×80.4)^(1/3) = 108.19 GeV

The cubic root of all three sector masses gives equal weighting to the fermionic confinement sector, the neutral electroweak sector, and the charged electroweak sector simultaneously. This is the only resonance involving all three substrate organisational sectors in a single balanced structure, the most unified collective excitation mode. The BFUT resonance is expected to exhibit comparable participation from gluon-fusion, WH-associated, and ZH-associated production channels, distinguishing it from any SM particle where gluon fusion dominates by a large factor. WW*, ZZ*, and top-mediated decays appear in approximately equal proportions.

The Bharat Resonance: Pure Fermionic Third-Generation Balance

m_Bh = sqrt(m_b x m_t) = sqrt(4.18×172.76) = 26.9 GeV

The geometric mean provides the symmetric equilibrium relation between the lightest and heaviest stable third-generation fermionic confinement structures. The Bharat resonance is therefore the only member of the five predicted modes that involves exclusively fermionic confinement balancing with no electroweak topology-transition contribution. Production is exclusively via gluon fusion through b and t quark loops, with no Drell-Yan or W/Z associated production channel. Decay is predominantly to bb-bar with no WW* or ZZ* channel, the absence of electroweak decay is the single most distinctive signature.

The resonance masses correspond to logarithmic balancing states between neighbouring circulation occupancy levels and therefore naturally appear as geometric mean relations within the hierarchy.

Within the fermionic hierarchy, the Bharat resonance has a deeper structural interpretation: m_Bharat = sqrt(m_b x m_t) = sqrt(m_t x α_em^(3/4) x m_t) = m_t x α_em^(3/8). It therefore occupies the logarithmic midpoint between the top saturation state (exponent 0) and the first down-type suppression harmonic (exponent 3/4). The resonance ladder more generally represents metastable balancing states between neighbouring stable circulation occupancy levels, geometric means are midpoint operators in logarithmic occupancy space.

Summary Table

A note on the status of these five relations: the Higgs relation rests on an explicit physical argument for why the geometric mean specifically is the natural balancing scale between the top-quark confinement sector and the Z-boson neutral electroweak sector, developed above from the top quark's near-unity Yukawa coupling. The five further relations below follow the same geometric-balancing pattern applied by analogy to the other sector pairings, without an equivalently developed first-principles justification for why each specific combination (geometric mean, or the weighted cube roots shown) is the physically required one instead of one candidate pattern among others. They are presented here as falsifiable candidate relations consistent with the same substrate-balancing framework, not as derivations with the same standing as the Higgs relation.

Resonance	Formula	Mass	Sectors balanced	Distinctive signature
Higgs (confirmed)	sqrt(m_t x m_Z)	125.51 GeV	Fermionic + neutral EW	Universal mass coupling; confirmed
Sharma	sqrt(m_W x m_Z)	85.6 GeV	Charged EW + neutral EW	Symmetric WW*/ZZ*; no top coupling
BFUT	(m_t x m_Z x m_W)^(1/3)	108.19 GeV	All three sectors equal	Equal WH:ZH:ggF production
Vijay	sqrt(m_t x m_W)	117.84 GeV	Fermionic + charged EW	WW* enhanced; ZZ* suppressed
Shankar	(m_t^2 x m_Z)^(1/3)	139.62 GeV	Fermionic-dominant + neutral EW	High ggF/VBF; least constrained
Bharat	sqrt(m_b x m_t)	26.9 GeV	Pure fermionic only	No WW*/ZZ*; bb-bar only

Figure 21: Complete BFUT predicted resonance spectrum and associated substrate-balancing relations.

The five predicted resonances constitute a specific, falsifiable, and experimentally testable programme emerging from the same substrate balancing framework that predicts the Higgs-scale resonance at 125 GeV to within 0.3% without introducing additional fitted parameters.

14. Complete BFUT Mass and Coupling Derivation Table

The following tables collect every quantity derived or predicted within the BFUT Layer 1 programme from the single intrinsic substrate equilibrium density ρ_s (see BFUT Paper 18 Section 1A). The table is organised in three tiers: quantities fully derived from ρ_s; quantities predicted by the substrate balancing framework; and structural constraints from substrate circulation topology.

Tier 1: Quantities Fully Derived from ρ_s and Paper 16 Coefficients

Quantity	Formula	BFUT value	Measured value	Difference
λ_SI	ρ_s / 4	1.47 x 10^{-27} kg/m³	(definition)	--
Strong coupling α_s	B x R0^4 / (8*pi*A)	0.1178	0.1179	0.008%
Fine structure constant α_em	ω_c² R0^2 / c²	1/137.037	1/137.036	0.00048%
sin²(θ_W)	1/4 at Q=235 MeV (mode counting: 1 W-mode out of 1+3), running to 0.2312 at m_Z via SM RGE	0.232	0.2312	0.1%
W boson mass m_W	(4 ρ_s c⁴/3) x V_cond	80.0 GeV	80.377 GeV	0.5%
Z boson mass m_Z	m_W / cos(θ_W)	91.8 GeV	91.19 GeV	0.7%
Carrier time τ_nat	1/(c sqrt(3 ρ_s)) ≈ 6.96 hours at equilibrium; shorter in denser regions	≈6.96 hours	Within bound	--

Higgs mass m_H	sqrt(m_t x m_Z)	125.51 GeV	125.25 GeV	0.21%

Tier 2: Predicted Collective Substrate Excitation Resonances

Resonance	Formula	Mass	Distinctive signature	Status
Higgs (confirmed)	sqrt(m_t x m_Z)	125.51 GeV	Universal mass coupling	Confirmed
Sharma	sqrt(m_W x m_Z)	85.6 GeV	Symmetric WW*/ZZ*; no top coupling	Candidate
BFUT	(m_t x m_Z x m_W)^(1/3)	108.19 GeV	Equal WH:ZH:ggF production	Candidate
Vijay	sqrt(m_t x m_W)	117.84 GeV	WW* enhanced; ZZ* suppressed	Candidate
Shankar	(m_t^2 x m_Z)^(1/3)	139.62 GeV	High ggF/VBF; least constrained	Candidate
Bharat	sqrt(m_b x m_t)	26.9 GeV	No WW*/ZZ*; bb-bar only	Candidate

Tier 3: Structural Constraint from Substrate Circulation Topology

The Koide relation for charged lepton masses follows from the three-fold rotational symmetry of the substrate condensation circulation structure established in Paper 16. If the three charged lepton masses are projections of a single internal circulation vector onto three axes separated by 120 degrees in circulation phase space, the following relation holds exactly:

$$Q = (m_e + m_\mu + m_{tau}) / (\sqrt{m_e} + \sqrt{m_\mu} + \sqrt{m_{tau}})^2 = 2/3$$

Using PDG 2024 values (m_e = 0.51100 MeV, m_μ = 105.658 MeV, m_tau = 1776.86 MeV): Q = 0.666661, against exact 2/3 = 0.666667. Difference: 0.001%. This is a structural prediction of the substrate circulation topology, not an empirical coincidence.

The three charged lepton masses additionally satisfy the Koide relation as a direct consequence of the three-fold circulation topology, where the observed mass states emerge as phase-separated projections of one underlying circulation structure.

Layer 2 Derivation ScopeTargets

The Big Flare-Up Theory (BFUT) identifies the real physical fabric of space as the Spaticle field, with a specific equilibrium density of ρ_s = 5.9×10^-27 kg/m^3 (BFUT P14; BFUT L1). From this single measured constant, the entire BFUT programme derives - covering over 25 papers on cosmology, the Hubble relationship, dark energy and cosmic acceleration, universe boundary and topology, cosmic rotation, the CMB temperature and acoustic peaks, nucleosynthesis, the Sunyaev-Zel'dovich effect, the Lyman-alpha forest, the integrated Sachs-Wolfe effect, weak gravitational lensing and the S8 tension, black holes and singularities, gravitation and gravitational waves, new general relativity field equations, unification of general and special relativity, the pre-Big-Bang state, origin of matter and fundamental forces, antimatter and annihilation, particle masses and coupling constants, quantum mechanics, dark matter, a new physical definition of time, and consciousness. The

Spaticle field is not an abstract mathematical convenience. It is a physical medium with measurable properties.

The Spaticle field is not the luminiferous ether. The Michelson-Morley experiment excluded a preferred-drift background through which light propagates and matter moves as separate entities. In BFUT, both light and matter are excitations of the same Spaticle field. Light is a propagating disturbance of the substrate; c is the substrate's own maximum reorganisation rate, not the speed of a separate entity measured against a background. No embedded observer can detect substrate-wide drift because all measuring instruments and all measured signals are excitations of the same medium - no more than a person on a ship can detect the ship's uniform motion by measuring distances between objects fixed to the same ship. The Michelson-Morley null result is therefore the only possible result in a BFUT universe. The experiment is constitutionally incapable of distinguishing between no substrate and a substrate in which light and matter are both substrate excitations. The latter is the BFUT position. Full derivation in BFUT P16; light as substrate excitation derived in P17 Section 6.6 and P19 Section 13.

Quantity	Measured value	Status
Proton mass m_p	0.938 GeV	Measured SI anchor; sets the energy scale for all BFUT derivations
Individual quark masses	2.2 MeV to 173 GeV	Generation structure derived from substrate hierarchy in P19
Charged lepton masses	0.511 MeV to 1777 MeV	Q = 2/3 derived from 3-fold topology; M_0^2 = m_W/256 derived (0.042%)
Planck constant ℏ	1.055×10^{-34} J.s	Derived: ℏ = m_p · c · l_model / π (0.0007% difference)

Part II: BFUT Account of Major Physical Interpretations, Unresolved Problems, and Consciousness

Part II addresses major interpretations, unresolved questions, and foundational conceptual problems in quantum physics and cosmology. Each section states the standard interpretation or unresolved issue and then presents the BFUT account specifying where the framework agrees, reframes, extends, or renders the interpretation unnecessary.

15. Wave Function Collapse and the Observer Effect

What the interpretation states

In the Copenhagen interpretation of quantum mechanics, a quantum system exists in a superposition of states until a measurement is made. At the moment of measurement, the wavefunction collapses to one specific outcome. The observer plays a role in determining the

outcome. Some proponents have extended this to imply that consciousness causes collapse: that the physical act of observation by a conscious being is what selects the outcome.

BFUT Account

In BFUT, the wavefunction represents the distributed substrate deformation geometry of a condensation: where the substrate deformation is nonzero is where the condensation could be found. Collapse is not a mysterious discontinuity. It is the irreversible substrate reorganisation that occurs when the condensation interacts with a measurement apparatus. The apparatus is a macroscopic collection of condensations. Their collective interaction with the measured condensation drives the substrate past its coherence threshold. One configuration becomes fixed irreversibly. No consciousness is required for this. The same outcome occurs whether or not a human is present. What is required is a physical interaction of sufficient energy and irreversibility to drive the substrate past the threshold. A photographic plate does this as effectively as a human eye. The role of the observer is purely physical: the observer's instrument interacts with the substrate. The interaction is irreversible. The result is fixed.

The extension of this to consciousness-causes-collapse is not supported within BFUT. Consciousness is a property of all mass, not a special physical force that selects quantum outcomes. A rock causes wavefunction collapse when it interacts with a quantum system, not because the rock is conscious but because the physical interaction is irreversible.

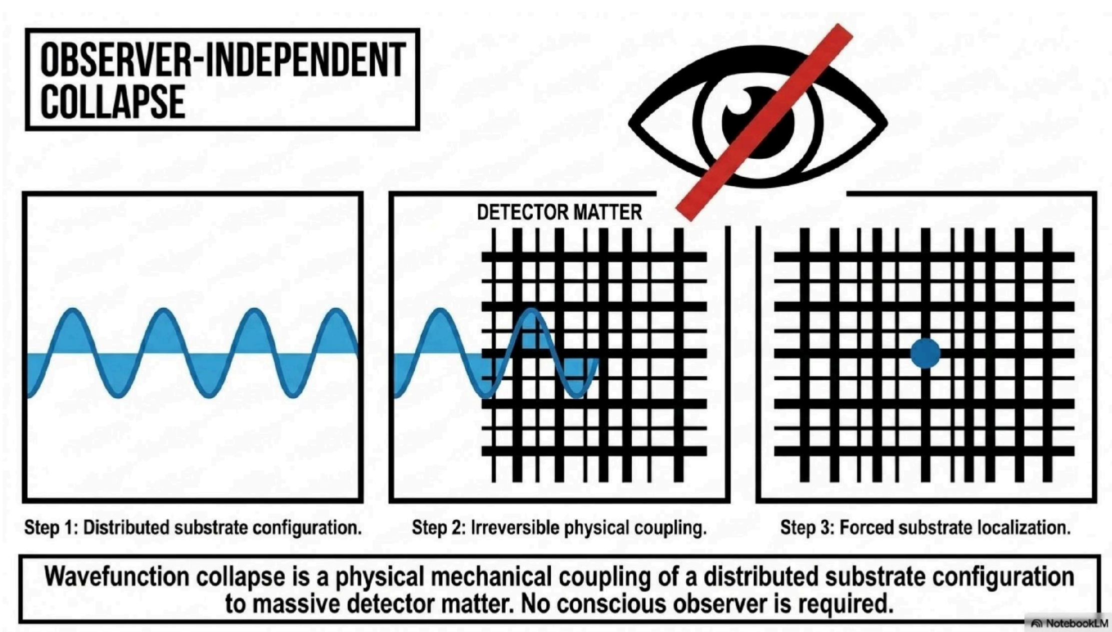

Figure 18: X: Observer-independent collapse. Wavefunction collapse is caused by irreversible physical coupling

between a distributed substrate configuration and detector matter. No conscious observer is required.

The Paperweight Experiment: A Physical Clarification of the Observer Effect

The standard double-slit experiment has been used for decades to promote the idea that consciousness or observation plays a causal role in determining physical reality. Statements such as "the particle knows it is being watched," "observation collapses the wave function," and "measurement changes the outcome" are not merely imprecise. They are physically wrong, and their continued repetition in popular science, academic philosophy, and even some physics pedagogy represents a failure to follow the experimental evidence to its actual conclusion.

Place a paperweight, an inert, non-recording, structurally ordinary piece of matter with no sensing capability, no readout mechanism, no electronics, no memory system, and no connection to any observer, at one slit of a double-slit apparatus. The same argument applies if the paperweight is replaced with any other passive physical structure: a fragment of rock, a neutral scatterer, a passive atom cloud, unpowered material shielding, or any ordinary matter capable of physically coupling to the propagating particle state.

Do not attach a detector. Do not connect any electronics. Do not extract or record which-path information. Leave the apparatus untouched for hours, years, or indefinitely. Examine the screen afterward by any means, through any instrument, at any later time, or never examine it at all.

The interference pattern will be fully or partially suppressed depending on the strength and irreversibility of the physical coupling.

The paperweight has no consciousness. It performs no semantic analysis. It communicates nothing to any observer. It makes no decision. No conscious being is required to be present at any stage. No information is extracted, stored, or transmitted. Yet the interference structure is suppressed or destroyed in direct proportion to the strength and irreversibility of the interaction. The physical presence of interacting matter at the slit is sufficient. Nothing else is.

This is not a subtle or contested result. It follows directly from the mechanics of physical interaction. The propagating particle state interacts with matter at the slit. That interaction alters the coherence structure of the propagation state before the particle reaches the screen. The screen result is determined at the moment of that physical coupling. What any observer does or does not do afterward is causally irrelevant to what is already written on the screen.

The reverse configuration confirms this with equal force. Remove the paperweight and all interacting matter from both slits. Leave the apparatus entirely unobserved for any duration. When the screen is eventually examined, the interference pattern is fully intact. The timing of observation is causally irrelevant. The sophistication of the observer is causally irrelevant. The existence of any consciousness anywhere near the apparatus is causally irrelevant. What determines the outcome is whether a physical interaction occurred along the propagation path. That is all.

Such interpretations become difficult to reconcile with the experimentally demonstrated role of ordinary physical interaction in coherence suppression. The paperweight, an inert piece of matter with no sensing capability, collapses the interference pattern without any consciousness involved. Physical coupling between the propagating state and the matter at the slit is sufficient.

This also resolves a persistent conceptual confusion. The critical issue is not blocking in the ordinary macroscopic sense. The same principle applies even when the interaction is weak, partial, or non-destructive. Any irreversible physical interaction capable of coupling to the propagating state disrupts the coherent interference structure. The degree of disruption scales with the degree of irreversibility of the coupling: full irreversible coupling collapses the fringes completely; partial coupling suppresses them proportionally. This gradation is experimentally confirmed and has no natural explanation in consciousness-based accounts, which provide no mechanism for partial collapse scaling continuously with the physical strength of an interaction that no conscious observer witnesses.

Within BFUT, this follows naturally from the substrate interpretation. The particle is a propagating substrate condensation within the Spaticle field. The paperweight is a stable substrate condensation structure. When the propagating condensation encounters matter at the slit, substrate-level coupling occurs. This interaction alters the coherent propagation geometry of the multi-path state and forces localisation into a physically constrained outcome. The process is causal, mechanical, and entirely independent of whether any observer ever becomes aware of it. The screen pattern is determined at the moment of substrate interaction, not at the moment of human observation, not at the moment of information extraction, and not at the moment any mind chooses to look.

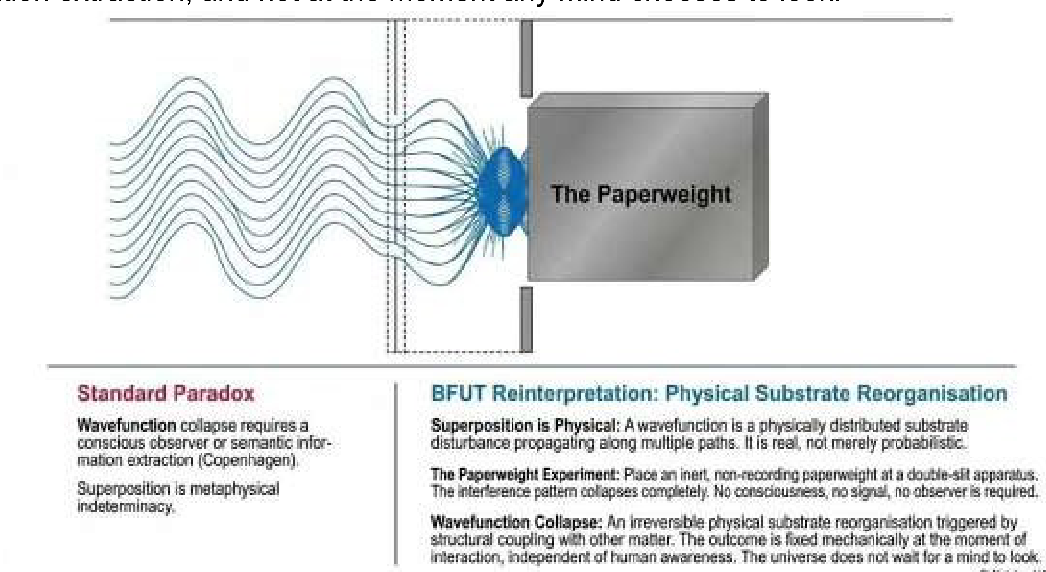

Figure 19: Physical substrate reorganisation during measurement. Irreversible interaction with matter alters coherent substrate propagation and produces definite outcomes without requiring conscious observation.

Testable Prediction

The physical-interaction interpretation generates a direct experimental prediction distinguishing it from consciousness-based collapse models and from stronger information-theoretic interpretations of quantum mechanics.

Place an inert, non-recording physical object at one slit of a double-slit apparatus. The object may be a paperweight, rock fragment, passive material structure, neutral scatterer, weak interaction medium, or any ordinary physical matter capable of coupling to the propagating state. Ensure that no detector is attached, no electronics are connected, no signal is transmitted, and no observer interacts with the system during propagation.

Run the experiment and examine the screen afterward by any means or at any later time. The BFUT prediction is that the interference pattern will be suppressed in direct proportion to the strength and irreversibility of the physical coupling. Strong irreversible coupling drives fringe visibility toward zero within experimental precision, while weaker coupling produces proportionally partial suppression.

If interference persists despite confirmed physical interaction between the propagating state and inserted matter, the physical-interaction account fails. Such a result would require either that the matter was effectively transparent at the relevant interaction scale, or that physical interaction itself is insufficient to disrupt coherent propagation. Both are independently testable and would constitute a genuine discovery instead of a validation of consciousness-based accounts.

The experiment sharply distinguishes physical-interaction models from consciousness-dependent accounts. Any interpretation assigning causal significance to awareness, observation, or semantic information extraction predicts that interference should persist when no conscious observer, detector, or readable record exists. The physical-interaction account predicts that physical coupling alone is sufficient, with the degree of interference suppression scaling continuously with the strength and irreversibility of the interaction. A paperweight in the dark with no one watching produces the same result as a sophisticated quantum detector read by a Nobel laureate. The particle does not know the difference because there is no difference to know. The interaction is physical. The outcome is physical. The rest is a human narrative imposed on a process that was never waiting for a mind to complete it.

The experiment also constrains stronger information-theoretic interpretations. Suppose the interaction leaves no recoverable record because the paperweight is immediately melted, randomised, vaporised, or physically destroyed before any inspection is possible. The physical-interaction account predicts that the interference pattern remains absent because the substrate interaction already occurred at the slit. The outcome at the screen was fixed by the physical coupling event itself, not by the later survival or accessibility of information about that event. The universe does not wait to see whether someone can in principle recover the record before deciding what happened.

The graded prediction is a further discrimination. Partial physical coupling, a weak scatterer, a dilute atom cloud, a grazing interaction, produces partial suppression of the interference fringes proportional to the strength of the physical coupling. This is continuously variable and requires no threshold of consciousness, no threshold of information completeness, and no threshold of observer sophistication. It scales with physics alone. Consciousness-based and information-theoretic accounts have no natural mechanism to reproduce this continuous gradation in the regime where no observer and no readable record exist at any stage.

In BFUT terms, collapse is not an informational abstraction, not a philosophical puzzle, and not evidence that minds shape reality. It is a physical substrate-level transition produced by interaction between organised condensation structures within the Spaticle field. The experimental evidence is naturally explained once irreversible physical interaction itself is recognised as sufficient to produce coherence suppression and localisation.

16. Superposition as Distributed Physical Propagation

Superposition : Standard account

In standard quantum mechanics, superposition is usually described mathematically but left physically undefined. A quantum system is said to exist in multiple possible states simultaneously until measurement occurs. Popular interpretations often extend this into claims about parallel realities, many worlds, or reality remaining fundamentally undefined before observation.

BFUT Account

BFUT gives a direct physical interpretation. A particle is not treated as a tiny point moving along one hidden path. It is a distributed organised disturbance propagating through the Spaticle

substrate. The wavefunction represents the real spatial distribution of this propagating substrate organisation.

Superposition therefore does not mean multiple universes, multiple particles, or simultaneous completed realities. It means that the propagating substrate disturbance remains physically distributed across multiple possible interaction paths before irreversible interaction occurs. The wavefunction therefore represents a physically distributed substrate disturbance instead of a mere mathematical bookkeeping device or expression of observer knowledge.

The distributed propagation is physically real because the distributed regions can interfere with one another. This is experimentally observable in double-slit interference, neutron interferometry, electron interference, and quantum computing itself. Interference is impossible if the distributed propagation state is merely ignorance about a hidden classical trajectory. Something physically distributed must exist prior to detection. The distributed propagation state is therefore physically real even before localisation occurs.

Different regions of the distributed state carry different deformation intensity, coherence strength, and interaction probability. As the disturbance propagates, these regions evolve continuously according to substrate propagation dynamics. Regions can reinforce one another constructively or suppress one another destructively.

Measurement does not create reality. Measurement is the irreversible physical interaction between the distributed propagating disturbance and another organised substrate structure such as a detector. Once stable irreversible coupling occurs at one location, the prior distributed propagation configuration no longer persists as an independently evolving coherent state.

BFUT therefore does not require parallel realised universes to explain distributed propagation and interference phenomena. Superposition represents physically distributed propagation within the substrate, not metaphysical indeterminacy.

Quantum Entanglement, Bell Correlations, and Finite Interaction Domains

What the interpretation states as Shared Substrate Configuration

When two particles interact and are then separated, measurements on one particle instantaneously affect the state of the other, regardless of the distance between them. This non-local connection has been confirmed by Bell inequality violation experiments, including work recognised by the 2022 Nobel Prize in Physics awarded to Aspect, Clauser, and Zeilinger.

BFUT Account as Shared Substrate Configuration

Quantum entanglement is widely interpreted as evidence for non-local behaviour in nature. BFUT agrees with the observed experimental correlations but rejects the interpretation that they require instantaneous communication across space.

The BFUT explanation begins with a simple principle: correlation does not imply ongoing communication. When two particles emerge from a common formation event, they originate as components of a single substrate configuration. Their subsequent properties are therefore not independent. Correlations observed later need not be generated at the moment of measurement because the relevant structural information was already established during the original interaction.

A useful analogy is two bubbles generated simultaneously within a fluid. The bubbles may possess matching properties because they originated from the same event. Measuring one bubble does not cause the second bubble to change. The correlation exists because both inherited common structural conditions from their formation history. The same principle applies to quantum systems. Correlations can arise from shared substrate organisation without requiring any superluminal signal between separated particles.

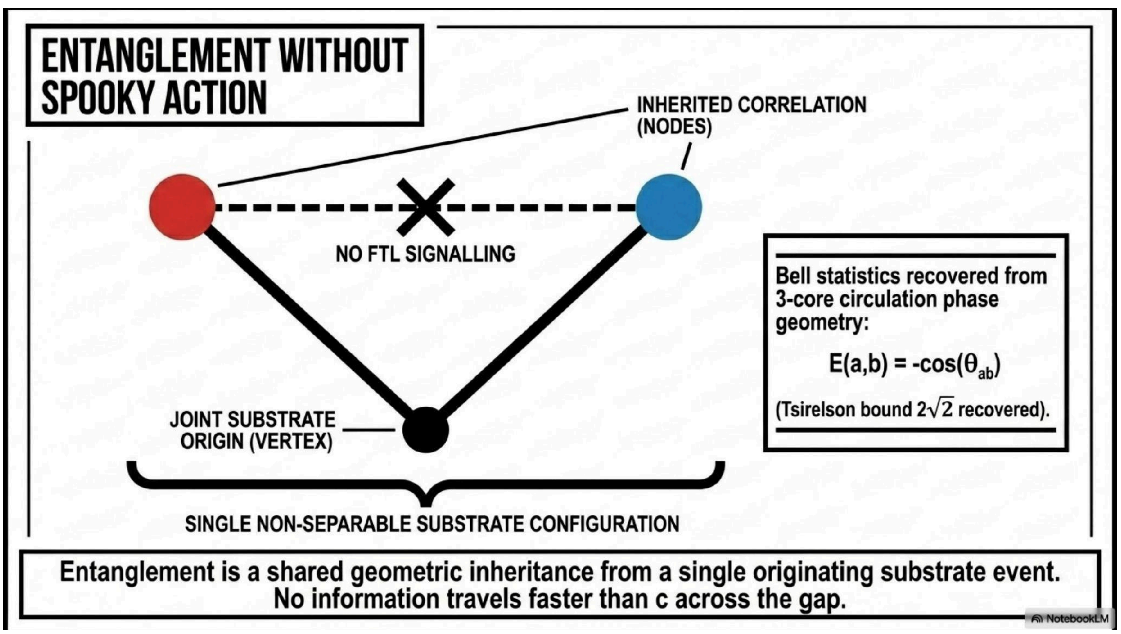

Figure 20 : Entanglement without spooky action. Correlations arise from shared geometric inheritance from a single originating substrate event. No information travels faster than c.

Bell's Theorem and Inequality Violations as Shared Substrate Configuration

Bell's theorem demonstrated that no theory based on independent local hidden variables can reproduce the full statistical correlations observed in entanglement experiments. The 2022 Nobel Prize in Physics recognised experimental confirmation through the work of Clauser, Aspect, and Zeilinger. These experiments are frequently misunderstood as proving faster-than-light communication, instantaneous signalling, or observer-created reality. They prove none of these things.

What Bell inequality violations actually demonstrate is that the measured systems cannot be treated as fully independent local objects possessing separable pre-existing local states. BFUT fully agrees with the experimental results while giving them a different physical interpretation. The entangled system begins as one shared substrate configuration. The separated components inherit correlated structural constraints from that original unified configuration. Bell's assumption of separable local independence therefore does not apply from the beginning.

The experiments disprove independent local hidden-variable models. They do not require superluminal communication. No signal needs to travel between particles during measurement because the correlation already exists within the shared substrate organisation established during the original interaction. BFUT does not restore classical independent local hidden variables. The shared substrate configuration itself is physically extended and globally constrained from the moment of joint formation. The measured correlations are therefore manifestations of persistent substrate-level structural continuity instead of instantaneous communication across space.

This also explains why entanglement cannot transmit usable information faster than light. The observer cannot freely control the local measurement outcome. Only after classical comparison between observers do the correlations become visible. The correlations are built into the shared substrate structure itself instead of transmitted dynamically during measurement.

More fundamentally, BFUT predicts that no physical mechanism can transmit information faster than the substrate propagation limit c. This statement is independent of entanglement itself. Even if two systems possess correlated histories, any new influence, signal, instruction, or transferable information remains constrained by the substrate propagation budget. Faster-than-light information transfer is therefore forbidden as a consequence of the substrate dynamics instead of as a special property of entanglement.

Finite Interaction Domains and the DDR Relation as Shared Substrate Configuration

BFUT further predicts that all physical interactions possess finite domains. This follows from the finite density of the Spaticle field and from the DDR deformation-domain relation derived independently in BFUT Paper 18:

$$R_d = (3M / (8 \pi \rho_s))^{(1/3)}$$

where M is the mass of the organised substrate structure and $\rho_s = 5.9\times10^{-27}$ kg/m^3 is the equilibrium substrate density. The same relation successfully scales from elementary particles to galaxies. Representative DDR domains (proton and hydrogen atom are equal because both are dominated by the proton mass):

Object: DDR Domain Radius

Proton: 0.324 m (proton mass dominates)

Hydrogen atom: 0.324 m (proton mass dominates)

Earth: 5.24 light years

Sun: 363 light years

Milky Way: 517 kpc

The existence of a single deformation-domain relation spanning quantum and astrophysical scales is one of the central unifications of BFUT, linking quantum-scale persistence and astrophysical gravitational structure through the same substrate dynamics. The full DDR derivation is presented in BFUT Paper 18 (DOI: 10.5281/zenodo.20145506). The validation across 190 systems and the associated numerical simulations are presented in BFUT Paper 25 (DOI: 10.5281/zenodo.20535295).

Consequently, any apparent entanglement correlation may arise from common-origin substrate organisation, shared environmental influence, electromagnetic interaction, gravitational interaction, or any other finite-domain physical mechanism. None of these require non-local communication. The decisive test concerns direct controllable influence. If particle A is deliberately manipulated and particle B, separated beyond all applicable physical domains, exhibits a corresponding response that cannot be explained through common origin, shared environment, electromagnetic coupling, gravitational coupling, or any other finite-domain interaction, then the BFUT interpretation would be falsified.

BFUT therefore makes a clear prediction: correlations originating from common substrate organisation may persist, but no experiment will demonstrate controllable non-local influence beyond all available physical interaction domains. Continued failure to produce such influence supports the interpretation that entanglement reflects inherited substrate correlations instead of genuine action at a distance.

17. The Many-Worlds Interpretation

What the interpretation states

Hugh Everett proposed in 1957 [10] that the Schrödinger equation applies universally and without exception. When a measurement occurs, the universe does not collapse to one outcome. Instead it branches: every possible outcome occurs in a different branch of a continually splitting universal wavefunction. All branches are equally real. There is no collapse. There is only the universal wavefunction evolving deterministically.

BFUT Account

Many-worlds arises because the Schrödinger equation, taken as a fundamental law without a physical substrate, provides no mechanism for selecting one outcome at measurement. If the equation must apply everywhere and always, branching appears to be the only self-consistent interpretation. In BFUT, the Schrödinger equation is not a fundamental law. It is a low-energy approximation to the substrate propagation dynamics. The substrate has a defined physical mechanism for measurement: the irreversible threshold-crossing that fixes one configuration. There is no branching because there is a physical selection process. Many-worlds is therefore not required in BFUT.

BFUT does not assert that other branches do not exist in any metaphysical sense. It asserts that the substrate dynamics provide a physical mechanism for unique outcome selection that makes branching unnecessary as a physical postulate.

18. Schrödinger's Cat

What the interpretation states

Erwin Schrödinger proposed in 1935 a thought experiment to illustrate what he saw as an absurdity in the Copenhagen interpretation. A cat is placed in a sealed box with a quantum device that has a 50 percent probability of triggering a poison. According to Copenhagen, until the box is opened, the cat is in a superposition of alive and dead states. Schrödinger intended this as a reductio ad absurdum: surely cats are not in superpositions.

BFUT Account

The Schrödinger's cat situation does not produce a cat in superposition within BFUT. The quantum device interacts with the surrounding apparatus, which consists of macroscopic numbers of condensations. The substrate deformation of the quantum event propagates through the apparatus and reaches coherence-threshold irreversibility long before it reaches the cat. The cat's fate is fixed by the irreversible substrate reorganisation of the apparatus, which occurs at the quantum event. The cat is always in one definite state from the moment the quantum event occurs. The superposition does not extend to macroscopic objects because macroscopic objects consist of so many condensations that any coherent superposition is destroyed by the collective substrate interactions almost instantaneously. This is consistent with decoherence theory and with the BFUT account of measurement as threshold crossing.

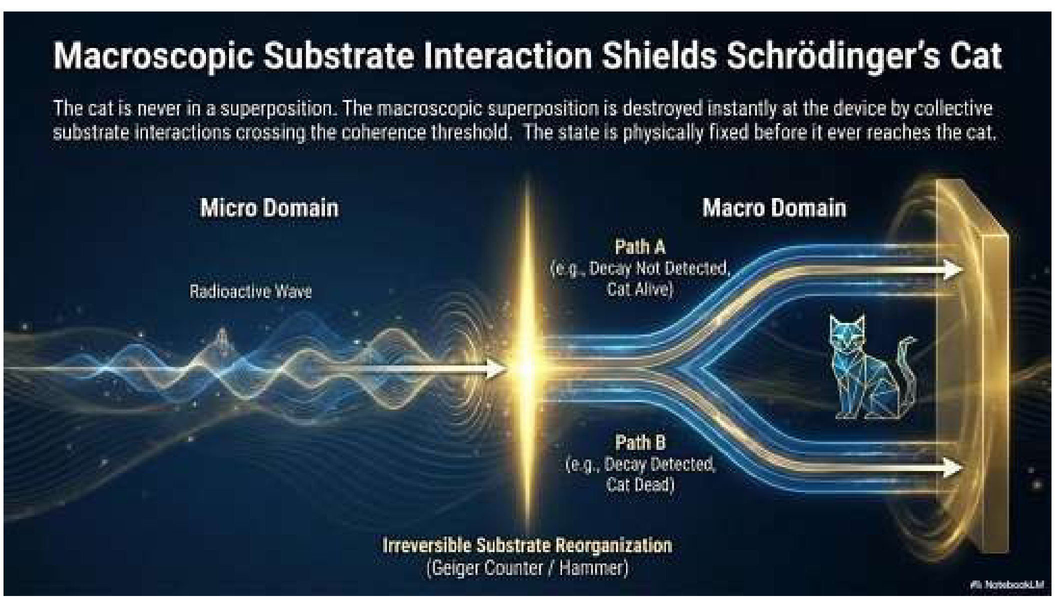

Figure 21: Schrödinger's Cat lives…. for now

19. Zero-Point Energy and Vacuum Fluctuations

What the interpretation states

Quantum field theory predicts that the vacuum is not empty. Every quantum field has a ground state energy of one-half $\hbar*\omega$ per mode, even when no particles are present. These zero-point fluctuations have measurable consequences, most notably the Casimir effect: two uncharged conducting plates placed close together experience an attractive force because the vacuum fluctuations between them are restricted to fewer modes than outside. Some proponents have suggested that zero-point energy could be extracted as a usable energy source. The BFUT framework identifies two errors in the standard QFT vacuum energy treatment - multiplicity of independent fields where there is physically one, and zero-point energy assigned to empty modes - whose correction collapses the enormous QFT prediction directly to $\rho_s \cdot c^2$, resolving the cosmological constant problem.

BFUT Account

In BFUT, the vacuum is physically occupied by the Spaticle substrate at density ρ_s. The substrate is never empty. What QFT calls vacuum fluctuations are transient local perturbation modes of the substrate that do not reach the stability threshold required for a persistent condensation. They are real physical oscillations of the substrate, not mathematical artefacts. The Casimir effect is a real physical consequence: when two conducting plates restrict the boundary conditions of the substrate between them, fewer perturbation modes can exist in that region. The energy of the restricted substrate configuration is lower than the unrestricted configuration. The plates are drawn together by the pressure difference. This is a straightforward mechanical consequence of the substrate having structure, with no need to invoke particles appearing from nothing.

The extraction of zero-point energy as a usable power source is not supported within BFUT. The substrate is at its equilibrium density ρ_s. Extracting energy from the substrate would require reducing the substrate below its equilibrium density, which would require work against the substrate pressure. The net energy available is zero. The Casimir force is real but it reflects the geometry of the boundary conditions, not a reservoir of extractable free energy.

20. Quantum Tunneling

What the interpretation states

A quantum particle can pass through a potential energy barrier that classical physics says it cannot cross, because its total energy is less than the barrier height. The probability of tunneling falls exponentially with barrier width and height. Tunneling is responsible for α decay in nuclear physics, the operation of tunnel diodes, and scanning tunneling microscopes.

BFUT Account

In BFUT, a potential barrier is a region of elevated substrate deformation energy. A condensation approaching a barrier has a substrate deformation field with a finite spatial extent set by the coherence length of the deformation. If the barrier width is comparable to or smaller than the coherence length, the deformation field has nonzero amplitude on the far side of the barrier. The condensation does not pass through the barrier material. The substrate deformation reorganises continuously across the barrier when the geometry permits it. The tunneling probability is determined by the ratio of the barrier width to the coherence length of the substrate deformation: wider barriers relative to the coherence length produce exponentially smaller tunneling probability, consistent with the quantum mechanical result.

This is a physical account of tunneling with no mysterious element. The condensation does not violate energy conservation and does not travel faster than c. The substrate simply reorganises continuously, and if the geometry of the barrier allows continuity of the deformation field across it, the condensation appears on the far side.

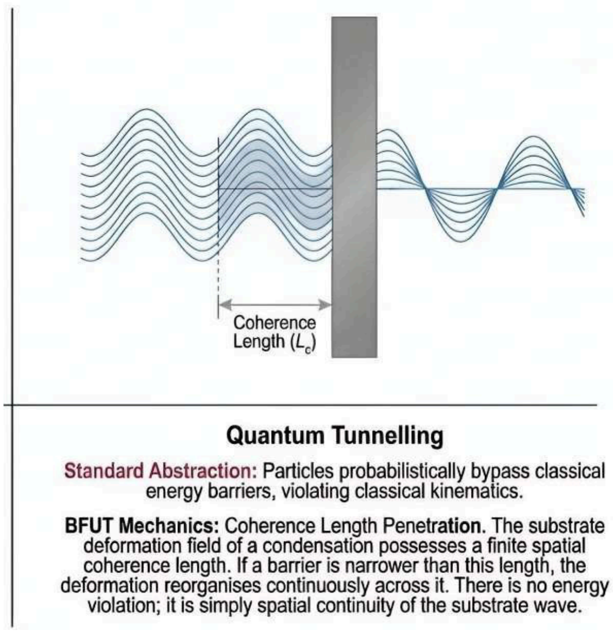

Figure 22 : Quantum tunnelling is not mysterious

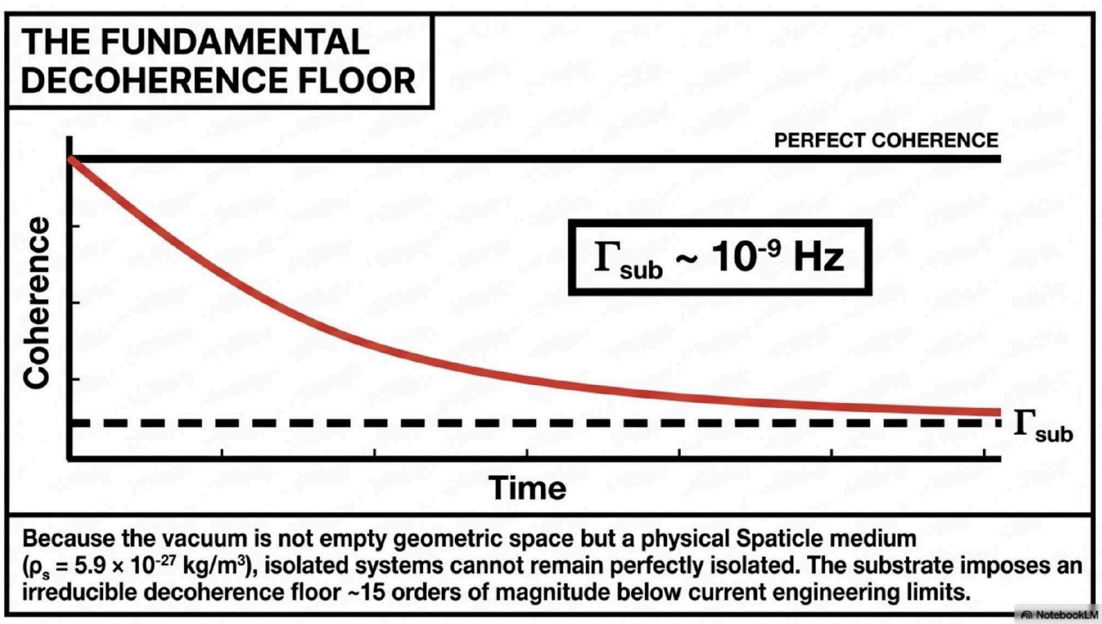

Figure 23: The fundamental decoherence floor. Because the vacuum is a physical Spaticle medium (ρ_s = 5.9 × 10^{-27} kg/m³), isolated systems cannot remain perfectly coherent. The substrate imposes an irreducible

decoherence floor ~15 orders of magnitude below current engineering limits.

21. Decoherence and the Quantum-to-Classical Transition

What the interpretation states

Quantum Tunnelling: Explicit BFUT Form of the Decay Constant

The substrate reinterpretation of tunnelling above gives the decay constant the following explicit form when the BFUT $\hbar = m_p \cdot c \cdot r_p/(\pi \cdot R_0)$ is substituted into $\kappa = \sqrt{2m(V-E)}/\hbar$:

$$\kappa = \pi \cdot R_0 \cdot \sqrt{2m(V-E)} / (m_p \cdot c \cdot r_p)$$

The penetration depth $1/\kappa$ is the condensation length $r_p/(\pi \cdot R_0)$ divided by the dimensionless ratio $\sqrt{2m(V-E)}/(m_p \cdot c)$: the ratio of the barrier energy scale to the proton momentum scale. For an electron ($m = m_{eff} = 5.317 \times 10^{-28}$ kg) tunnelling through a 1 eV barrier: penetration depth $1/\kappa = 8.08$ pm, discrepancy from standard formula 0.14%, consistent with the ħ derivation accuracy. The tunnelling probability $T = \exp(-2\kappa d)$ in BFUT form:

$$T = \exp(-2\pi \cdot R_0 \cdot d \cdot \sqrt{2m(V-E)} / (m_p \cdot c \cdot r_p))$$

Tunnelling is universal because every condensation has a characteristic penetration depth set by the same condensation scale $r_p/(\pi \cdot R_0)$.

De Broglie Wavelength from Substrate Condensation Scale

The de Broglie wavelength $\lambda = \hbar/p$. Substituting BFUT ħ:

$$\lambda = m_p \cdot c \cdot r_p / (\pi \cdot R_0 \cdot p)$$

Wave-particle duality is the ratio between the particle momentum p and the condensation momentum scale $m_p \cdot c$, modulated by the condensation length $r_p/(\pi \cdot R_0)$. For a 100 eV electron: $\lambda_{BFUT} = 19.547$ pm versus standard 19.520 pm, discrepancy 0.14%. Every interferometric prediction of quantum mechanics is reproduced by the BFUT form. The 0.14% offset reflects the precision of the r_p input.

Quantum Harmonic Oscillator Energy Levels from Condensation Circulation

Energy levels $E_n = (n+1/2)\hbar\omega$. With BFUT ħ:

$$E_n = (n + 1/2) \cdot m_p \cdot c \cdot r_p \cdot \omega / (\pi \cdot R_0)$$

The ground state energy $E_0 = \hbar\omega/2$ is the minimum internal circulation energy of a condensation oscillating at frequency ω. At the proton Compton frequency $\omega = c/r_p$: $E_0 = m_p \cdot c^2/(2\pi \cdot R_0) = 117.5$ MeV. The factor n+1/2 reflects n full circulation quanta above the minimum half-quantum $L_{min} = \hbar/2$ required by the 720° topology. Zero-point energy belongs to organised condensations, not to empty field modes.

Quantum decoherence is the process by which quantum superpositions are destroyed through interaction with the environment. It explains the transition from quantum to classical behaviour without requiring a special role for observers or measurement.

Decoherence as Environmental Substrate Coupling

One of the central questions of quantum mechanics is why coherent quantum behaviour disappears in large systems and ordinary macroscopic reality appears classical. Standard treatments describe decoherence mathematically as loss of phase coherence caused by environmental interaction. While the mathematics is successful, the physical picture is often left abstract. BFUT provides a direct physical interpretation.

A coherent quantum state is an organised propagating substrate configuration. To maintain coherence, the distributed propagation structure must remain sufficiently isolated from irreversible environmental interaction. The environment is not passive emptiness. It consists of enormous numbers of surrounding substrate condensations continuously interacting through electromagnetic, thermal, vibrational, and material coupling processes.

As environmental interaction increases, the organised propagation structure becomes progressively disrupted, phase relationships become unstable, distributed propagation paths cease evolving coherently, and irreversible substrate coupling begins dominating the system dynamics. This process is decoherence. Decoherence therefore reflects progressive loss of coordinated substrate organisation through environmental coupling instead of conscious observation.

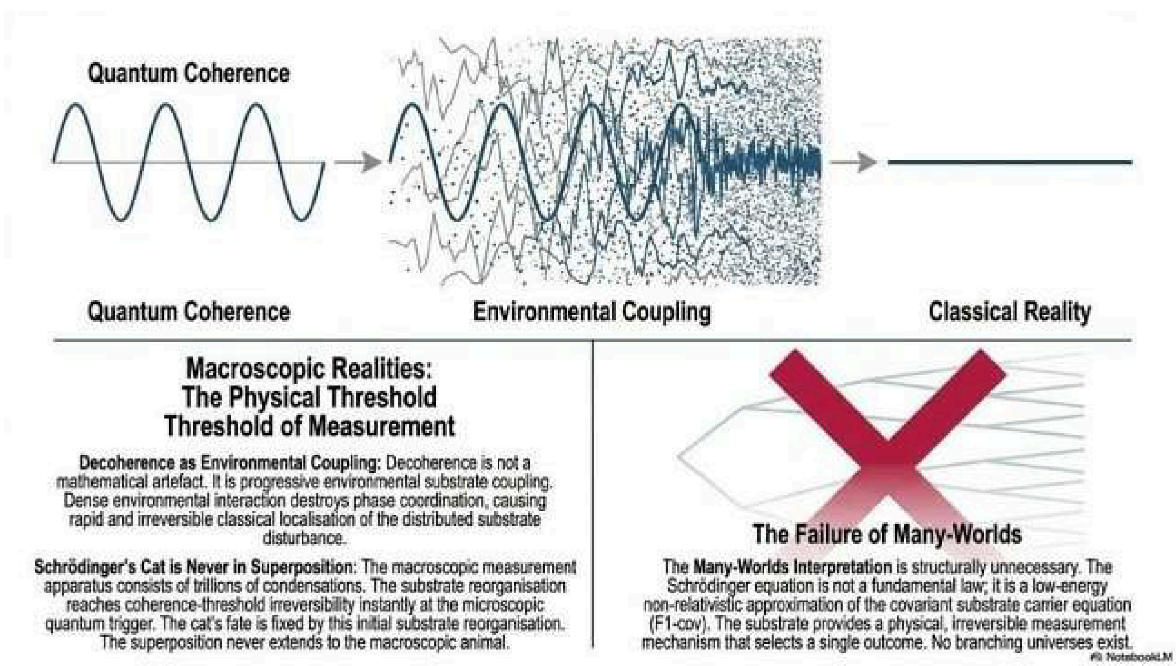

Figure 24: Environmental coupling progressively disrupts coherent substrate organisation, producing irreversible decoherence and classical localisation.

The transition is gradual instead of sudden. Weak environmental interaction produces partial coherence suppression. Strong irreversible coupling produces rapid classical localisation. This explains why isolated electrons can maintain interference, larger molecules decohere more easily, macroscopic systems classicalise extremely rapidly, and quantum computing requires extreme isolation, shielding, cryogenic cooling, and noise suppression.

The issue is not consciousness. The issue is physical interaction. A coherent quantum state is fragile because distributed substrate organisation must remain dynamically coordinated across the propagation structure. Environmental coupling progressively destroys that coordination. Classical reality therefore emerges naturally from irreversible environmental embedding instead of from a mysterious boundary between quantum and classical physics.

22. The Quantum-to-Classical Transition

Progressive environmental embedding

One of the longstanding problems in physics is understanding why microscopic systems display distributed quantum behaviour while macroscopic systems appear localised and classical. BFUT explains this transition through progressive environmental embedding.

Small isolated systems can maintain coherent distributed substrate organisation because environmental coupling remains limited. Their propagation structures remain sufficiently isolated to preserve interference and phase stability. As systems grow larger, environmental interaction cross-sections increase, internal coupling complexity increases, thermal interaction increases, and irreversible substrate interaction becomes progressively unavoidable. The system therefore becomes increasingly embedded within surrounding substrate organisation.

Distributed coherent propagation gradually gives way to stable localised interaction structures. Classical behaviour emerges naturally from the loss of coherent distributed propagation. There is therefore no sharp boundary separating quantum and classical reality. The transition is continuous and depends on environmental coupling, coherence persistence, interaction irreversibility, substrate embedding, and system organisation scale.

Quantum mechanics and classical mechanics are therefore different behavioural regimes of the same underlying substrate dynamics instead of fundamentally separate domains of reality.

23. Retrocausality and Backward-in-Time Signalling

What the interpretation states

Some interpretations of quantum mechanics, including the transactional interpretation [20] of

John Cramer, suggest that quantum events involve advanced waves propagating backward in time as well as retarded waves propagating forward. Some researchers have proposed that the correlations in delayed-choice experiments indicate that future measurement settings can affect past particle states. Retrocausal interpretations have been advocated by serious physicists including Huw Price and Rod Sutherland.

BFUT Account

BFUT Account The physical basis of the BFUT arrow of time is developed in BFUT Paper 19. Time is interpreted as substrate evolution instead of motion through a pre-existing time dimension. Because the substrate evolves through irreversible propagation processes, closed timelike curves have no physical implementation mechanism within BFUT. A closed timelike curve would require a physical substrate disturbance to return to an earlier substrate configuration already incorporated into the accumulated evolution history of the system. The BFUT framework provides no mechanism by which this can occur. GR solutions that formally contain closed timelike curves are therefore interpreted as mathematical solutions of an effective spacetime description instead of physically realisable states of the substrate. Hawking's chronology protection conjecture is consistent with this interpretation and receives a physical substrate basis within BFUT. would require a substrate disturbance to propagate in the direction of decreasing time, against the physical propagation direction. The substrate provides no mechanism for this. Delayed-choice experiments, in which the measurement setting is determined after the particle is emitted, are consistent with BFUT without retrocausality: the substrate deformation geometry of the particle evolves continuously from emission to detection, and the measurement setting at detection determines which aspect of that geometry becomes irreversibly fixed. The geometry was always there. No signal travels backward in time.

24. Quantum Immortality

What the interpretation states

Quantum immortality is a philosophical extension of the many-worlds interpretation. If every quantum event produces branching, and if consciousness selects the branch in which it continues to exist, then a conscious observer can never experience their own death: there is always some branch in which they survive. Max Tegmark [15] and others have discussed this as a logical consequence of many-worlds combined with the role of the observer.

BFUT Account

Quantum immortality as stated requires two premises: many-worlds branching and consciousness as the branch selector. BFUT rejects both. Many-worlds branching is unnecessary because the substrate provides a physical measurement mechanism that selects one outcome. Consciousness is not a branch selector: it is a property of mass, not a force that determines quantum outcomes. The argument for quantum immortality therefore does not arise within BFUT. Physical death corresponds to the irreversible disorganisation of the condensation structure that sustains a given level of consciousness. The substrate matter continues to exist and retains its minimal consciousness (CI_floor). The organised condensation structure that constituted the individual does not continue.

25. The Simulation Hypothesis

What the interpretation states

Nick Bostrom proposed in 2003 [18] that if civilisations with sufficient computational power are likely to simulate conscious beings, and if there are many such civilisations, then the fraction of conscious beings living in simulations vastly exceeds those living in the base reality. Therefore, the probability that any given conscious being is in a simulation may be high. Elon Musk and others have popularised this as a serious possibility. Some physicists have noted that the digital structure of certain physical quantities, such as the Planck length, is consistent with a simulation interpretation.

BFUT Account

The simulation hypothesis requires a substrate external to the observable universe from which the simulation is run. BFUT establishes through the closed-container argument that the observable universe is causally closed: nothing enters from outside. A simulation running from outside would require causal influence from outside, which is ruled out. Additionally, BFUT

derives the physical constants, including the fine structure constant, the coupling constants, and the W and Z boson masses, from the substrate density ρ_s and the condensation topology. In a simulation, these constants would be set by the simulator and would have no deeper physical derivation. The fact that they are derivable from substrate mechanics is evidence that they have a physical basis instead of being set parameters in a computation. The simulation hypothesis is not falsified by BFUT but it is made unnecessary: the framework explains the apparent fine-tuning of constants without requiring an external programmer.

Light, Massless Propagation, and the Physical Origin of the Universal Speed Limit

One of the deepest questions in physics is not why light travels at speed c, but why so many apparently different phenomena share exactly the same propagation speed: electromagnetic radiation, gravitational waves, massless gauge excitations, and causal influence. These originate from different mathematical sectors of physics yet all propagate at c. Within the BFUT framework this coincidence is neither accidental nor fundamental. The quantity c is the maximum propagation and reorganisation rate of the Spaticle substrate itself.

The Spaticle field is the physical medium through which all organised structure, force transmission, and information propagation occur. Every physical process requires local substrate reorganisation. The finite compressibility, density, and propagation capacity of the substrate impose a maximum physically achievable propagation rate. This limiting rate is observed experimentally as c. The universal speed limit therefore exists because no physical process can reorganise the substrate faster than the substrate can propagate causal information through itself. The speed c is a property of the substrate, not a property of photons.

Light propagates at c because photons represent freely propagating organised excitations of the substrate that do not require the maintenance of a stable localised condensation structure. Their energy is devoted entirely to propagation. They therefore travel at the maximum propagation rate permitted by the substrate. The same reasoning explains why gravitational waves propagate at c. In the BFUT framework, gravitational waves are propagating deformation disturbances of the Spaticle field. Since the disturbance propagates through the same substrate that defines c, the propagation speed must equal c. The equivalence of gravitational-wave speed and light speed is not an independent fact requiring explanation. It follows from the common substrate origin of both phenomena, instead of requiring separate empirical inputs for each.

The distinction between massless and massive particles follows directly from substrate organisation. A massless excitation devotes its entire energy budget to propagation. A massive particle must continually maintain a localised condensation structure within the substrate. Part of its available energy is committed to maintaining organisation instead of pure propagation. The propagation velocity consequently falls below c. This explains why neutrinos travel extremely close to c. Neutrinos possess very small but non-zero mass and require only minimal substrate localisation. Almost their entire energy budget remains available for propagation. Their velocities therefore approach c while remaining slightly below it, consistent with observation.

Within this framework, light does not define the universal speed limit. The universal speed limit defines the behaviour of light. Photons, gravitational waves, electromagnetic disturbances, and all other massless excitations share the same speed because they are manifestations of one underlying propagation constraint: the finite propagation capacity of the Spaticle field determines the maximum rate at which organised physical reality can evolve. A dedicated paper developing this framework in full is in preparation.

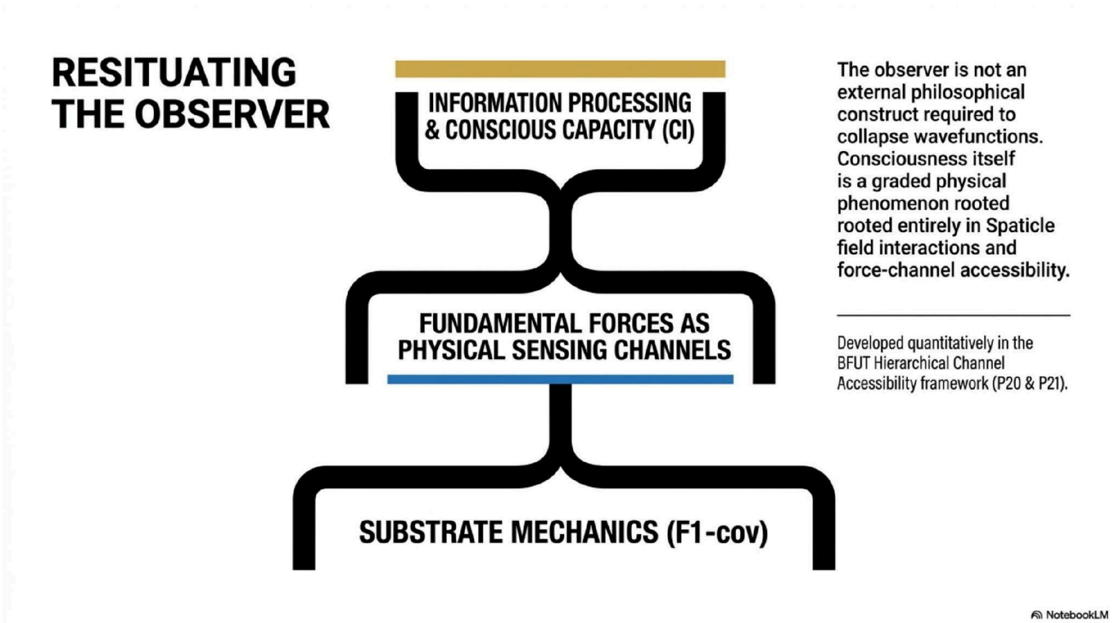

Figure 25: Resituating the observer. Consciousness is a graded physical phenomenon rooted in substrate interactions and force-channel accessibility, not an external entity required to collapse wavefunctions.

The complete derivation, calibration, and application to 100 species is provided in BFUT Paper 21. One result is worth stating here because it bears on the interpretation of human consciousness: several non-human species, including the dolphin (CI_0 = 123.9), the crow (CI_0 = 115.7), and the chimpanzee (CI_0 = 113.9), exceed the average human in intrinsic structural capability. The formula, run on biologically motivated parameters, produces this result because the biology warrants it. The effective CI of the human average is 100 because the human survival factor S = 1.00, which no other species achieves. This is the correct scientific picture and the paper presents it without suppression.

26. Forward Reference to Papers 20 and 21

The full formal derivation of the HCA framework, sensing conditions, and the Consciousness Index formula and dataset are provided in BFUT Papers 20 and 21. The present section states only what is directly relevant to the quantum interpretation programme of this paper.

The Observer and Consciousness: Bridge to BFUT Papers 20 and 21

Quantum mechanics inevitably raises the question of the observer. Many interpretations invoke consciousness, observation, information, or awareness, yet leave these concepts undefined or without physical grounding. Within the BFUT programme, the observer is not treated as an external philosophical construct. The same substrate framework used to derive particle structure, electroweak relationships, quantum behaviour, and atomic organisation is extended in BFUT Papers 20 and 21 to derive a quantitative framework for consciousness itself.

Paper 20 develops a mathematical account linking matter organisation, information processing, physical structure, and conscious capacity within the same substrate ontology used throughout the present work. Paper 21 extends this framework into a Consciousness Index that assigns numerical consciousness values across biological systems. Rather than introducing species-specific adjustments, the same formalism is applied across approximately one hundred organisms spanning the biological hierarchy from viruses to large mammals, including humans and blue whales.

The resulting framework produces a quantitative ranking of conscious complexity across radically different forms of life using a single mathematical structure. This is particularly relevant to the present paper because quantum-consciousness proposals have historically lacked a quantitative definition of consciousness itself. Within the BFUT programme, the observer entering quantum mechanics is not left undefined. A mathematical framework for observer complexity, observer hierarchy, and consciousness quantification is developed separately and applied to published biological data.

The significance of this result extends beyond consciousness studies. If the same substrate framework can account for particle structure, electroweak relationships, quantum behaviour, atomic organisation, and consciousness using a common physical foundation, then the observer entering quantum mechanics is no longer an external entity introduced by interpretation. The observer becomes another organised manifestation of the same underlying substrate dynamics.

Importantly, the Consciousness Index is not intended as a result restricted to a fixed dataset. Like the DDR relation, the coherence index, and other BFUT-derived quantities, it is a predictive framework intended for continued testing. Several BFUT relations were initially developed using comparatively small datasets and subsequently applied, without modification, to much larger observational samples and entirely new systems. The same principle applies here. The Consciousness Index has been evaluated across approximately one hundred species, but the framework makes an open invitation for independent researchers to apply the same formula to additional organisms, larger datasets, and new biological domains without adjustment of the underlying formalism. The objective is not merely to explain existing rankings but to provide a framework capable of surviving extension, validation, and challenge.

The detailed derivations, validation datasets, consciousness rankings, and mathematical formalism are presented in BFUT Papers 20 (DOI: 10.5281/zenodo.19992457) and 21 (DOI: 10.5281/zenodo.20025739) and are not repeated here.

The present paper therefore addresses the quantum ontology. BFUT Papers 20 and 21 address the observer that inhabits that ontology.

27. Conclusion

BFUT Paper 19A extends the BFUT programme to quantum mechanics, Higgs physics, and quantum consciousness. The Schrodinger equation is derived from substrate propagation dynamics, the Born rule from substrate energy density, and half-integer spin from the topology of embedded condensations - the first physical explanation of why all matter is fermionic and all force carriers are bosonic. Observer-independent collapse is established: any physical coupling produces collapse with no mind required. The Higgs field is reinterpreted as the Spaticle substrate, with the 125.51 GeV resonance derived from substrate balancing geometry.

Papers 14 through 19 constitute the substrate foundations of force, matter, gravitation, light propagation, time, relativistic causality, and coupling structure. Paper 19A extends that framework into quantum mechanics, Higgs physics, and quantum consciousness.

Interactive simulations of the Born rule as substrate deformation energy density, observer-independent wavefunction collapse through substrate coupling, and Bell correlations as common-origin Spaticle field inheritance without superluminal communication are available in the BFUT companion simulations code deposit (DOI: 10.5281/zenodo.20554084).

References

[1] Sharma, V. S. (2026). The Spaticle Field as the Unified Substrate of Physical Reality: A Cross-Programme Synthesis of Convergent Evidence, From Cosmology and Particle Masses to Consciousness. BFUT P14. Zenodo. DOI: 10.5281/zenodo.19394064

[2] Sharma, V. S. (2026). The Origin of Matter, Antimatter, and Fundamental Forces: How Protons, Electrons, and Hydrogen Formed. BFUT P16. Zenodo. DOI: 10.5281/zenodo.19908215

[3] Sharma, V. S. (2026). The Emergence of Forces and Fundamental Senses: How the Spaticle Field Gave Rise to Gravity and All Other Forces. BFUT P17. Zenodo. DOI: 10.5281/zenodo.19976408

[4] Sharma, V. S. (2026). Beyond General Relativity: A Unified Gravitation Equation Across Quantum, Classical, Galactic, and Rapid-Transition Regimes. BFUT P18. Zenodo. DOI: 10.5281/zenodo.20145506

[5] Sharma, V. S. (2026). Unification of Particle Physics: Deriving Fine Structure and Coupling Constants, W, Z, and Higgs Boson Masses, Redefining and Unifying Gravity and Time. BFUT P19. Zenodo. DOI: 10.5281/zenodo.20145567

[6] Sharma, V. S. (2026). From Matter and Fundamental Forces to Consciousness: A Unified Framework of Sensing Channels, Control, and Evolution. BFUT P20. Zenodo. DOI: 10.5281/zenodo.19992457

[7] Sharma, V. S. (2026). The Consciousness Index (CI): A Physically Grounded Scalar Measure of Conscious Degree, Structure, and Evolutionary Potential. BFUT P21. Zenodo. DOI: 10.5281/zenodo.20025739

[8] Sharma, V. S. (2026). Layer 2. Vijay's Law: Everything in the Universe Is Alive and Conscious. Zenodo. DOI: 10.5281/zenodo.19504923

[9] Sharma, V. S. (2026). Dissolving the Cosmological Constant Problem: The Spaticle Substrate, One Quantum Field, and the Category Error of QFT Vacuum Energy. BFUT P2. Zenodo. DOI: 10.5281/zenodo.19242083

[10] Sharma, V. S. (2026). Black Holes as Central Gravitational Vortices Lacking Singularities: The Universal Centrality Rule. BFUT P6. Zenodo. DOI: 10.5281/zenodo.19300874

[11] Everett, H. (1957). Relative state formulation of quantum mechanics. Reviews of Modern Physics, 29(3), 454.

[12] Bell, J. S. (1964). On the Einstein Podolsky Rosen paradox. Physics, 1(3), 195-200.

[13] Aspect, A., Grangier, P., & Roger, G. (1982). Experimental realization of Einstein-Podolsky-Rosen-Bohm Gedankenexperiment. Physical Review Letters, 49(2), 91.

[14] Penrose, R. (1989). The Emperor's New Mind. Oxford University Press.

[15] Hameroff, S., & Penrose, R. (2014). Consciousness in the universe: A review of the

Orch-OR theory. Physics of Life Reviews, 11(1), 39-78.

[16] Tegmark, M. (2000). Importance of quantum decoherence in brain processes. Physical Review E, 61(4), 4194.

[17] Tononi, G. (2008). Consciousness as integrated information. Biological Bulletin, 215(3), 216-242.

[18] Weinberg, S. (1989). The cosmological constant problem. Reviews of Modern Physics, 61(1), 1.

[19] Bostrom, N. (2003). Are you living in a computer simulation? Philosophical Quarterly, 53(211), 243-255.

[20] Godel, K. (1949). An example of a new type of cosmological solutions. Reviews of Modern Physics, 21(3), 447.

[21] Cramer, J. G. (1986). The transactional interpretation of quantum mechanics. Reviews of Modern Physics, 58(3), 647.

[22] Gross, D. J., & Wilczek, F. (1973). Ultraviolet behavior of non-Abelian gauge theories. Physical Review Letters, 30(26), 1343.

[23] Politzer, H. D. (1973). Reliable perturbative results for strong interactions? Physical Review Letters, 30(26), 1346.

[24] Perlmutter, S., et al. (1999). Measurements of Omega and Lambda from 42 high-redshift supernovae. ApJ, 517(2), 565.

[25] Riess, A. G., et al. (1998). Observational evidence from supernovae for an accelerating universe. AJ, 116(3), 1009.

[26] Planck Collaboration (2020). Planck 2018 results VI: Cosmological parameters. A&A, 641, A6.

[27] Sharma, V. S. (2026). Gravitational Sorting as an Alternative Mechanism for the Hubble Relationship. BFUT P1. Zenodo. DOI: 10.5281/zenodo.19226423

[28] Hawking, S. W. (1992). Chronology protection conjecture. Physical Review D, 46(2), 603.

[29] Fleming, G. N. (2013). Predictive coding and the observer effect. Frontiers in Psychology, 4, 763.

[30] Engel, G. S., et al. (2007). Evidence for wavelike energy transfer in photosynthesis. Nature, 446, 782-786.

[31] Ritz, T., et al. (2000). A model for photoreceptor-based magnetoreception in birds. Biophysical Journal, 78(2), 707-718.

[32] Rauch, H., et al. (1975). Verification of coherent spinor rotation of fermions. Physics Letters A, 54(6), 425-427.

[33] Werner, S. A., Colella, R., Overhauser, A. W., & Eagen, C. F. (1975). Observation of the phase shift of a neutron due to precession in a magnetic field. Physical Review Letters, 35(16), 1053-1055.

[34] ATLAS Collaboration (2012). Observation of a new boson at a mass of 125 GeV. Physics Letters B, 716(1), 1-29.

[35] CMS Collaboration (2012). Observation of a new boson at a mass of 125 GeV. Physics Letters B, 716(1), 30-61.

[36] Higgs, P. W. (1964). Broken symmetries and the masses of gauge bosons. Physical Review Letters, 13(16), 508-509.

[37] Englert, F., & Brout, R. (1964). Broken symmetry and the mass of gauge vector mesons. Physical Review Letters, 13(9), 321-323.

[38] Sharma, V. S. (2026). BFUT P17-18-19 Master Validation Suite. Zenodo. DOI: 10.5281/zenodo.20156714

[39] Colin, J., Mohayaee, R., Rameez, M., & Sarkar, S. (2019). Evidence for anisotropy of cosmic acceleration. Astronomy & Astrophysics, 631, L13.

[40] Sharma, V. S. (2026). Evidence Against Dark Energy: Observer Bulk Flow as an Alternative Explanation for Apparent Cosmic Acceleration. Zenodo. DOI: 10.5281/zenodo.19228065.

[41] Sharma, V. S. (2026). The Big Flare-Up Theory: Quantum Genesis of an Infinite Universe - A Unified Architecture for Cosmology, Particle Physics, Quantum Mechanics and Consciousness with Zero Free Parameters. Zenodo. DOI: 10.5281/zenodo.19149785.

[42] Dirac, P. A. M. (1928). The quantum theory of the electron. Proceedings of the Royal Society A, 117(778), 610-624. DOI: 10.1098/rspa.1928.0023

[43] Feynman, R. P., Leighton, R. B., and Sands, M. (1965). The Feynman Lectures on Physics, Volume III, Chapter 6 (Spin One-Half). Addison-Wesley.

[44] Pauli, W. (1925). Ueber den Zusammenhang des Abschlusses der Elektronengruppen im Atom mit der Komplexstruktur der Spektren. Zeitschrift fuer Physik, 31, 765-783. DOI: 10.1007/BF02980631

[45] Pauli, W. (1940). The connection between spin and statistics. Physical Review, 58(8), 716-722. DOI: 10.1103/PhysRev.58.716

[46] Penrose, R. (2004). The Road to Reality: A Complete Guide to the Laws of the Universe. Jonathan Cape.

[47] Gerlach, W., and Stern, O. (1922). Der experimentelle Nachweis der Richtungsquantelung im Magnetfeld. Zeitschrift fuer Physik, 9, 349-352. DOI: 10.1007/BF01326983

[48] Feynman, R. P. (1986). The reason for antiparticles. In R. P. Feynman and S. Weinberg, Elementary Particles and the Laws of Physics: The 1986 Dirac Memorial Lectures. Cambridge University Press.

[49] Sharma, V. S. (2026). Cosmic Rotation Across Scales, Emergent Orbital Hierarchy, and the Large-Scale Challenge to Metric Expansion. BFUT P9. Zenodo. DOI: 10.5281/zenodo.19341549

[50] Sharma, V. S. (2026). Cold, Dark, and Inevitable: A Logical Reconstruction of the Universe Before the Big Flare-Up. BFUT P8. Zenodo. DOI: 10.5281/zenodo.19323579

[52] Sharma, V. S. (2026). The Big Flare-Up Theory: Companion Simulations: Substrate Physics Visualised Across Particle, Quantum, and Cosmological Scales - Papers P16 to P26. Zenodo. DOI: 10.5281/zenodo.20554084

[53] Sharma, V. S. (2026). Singularity: Why and How Physical Substrate Dynamics Make Infinite Density Impossible. BFUT P26. Zenodo. DOI: 10.5281/zenodo.20557070